

Referee #1 comments: The manuscript by Benard et al. describes the results from a mesocosm experiment that was designed to investigate the responses of a natural phytoplankton community to warming and acidification. The authors observed a clear stimulation of phytoplankton growth by temperature whereas acidification had no or only a minor effect. Although many experimental studies have been conducted in recent years to investigate phytoplankton responses to warming or to acidification little is known about combined effects. The data provided by this study are thus potentially valuable and interesting. However, important information is lacking in the current version and need to be included and discussed to improve the value of this manuscript. The set-up of the experiment was designed to keep pH in the acidified mesocosms constant, yielding a decrease of pH after the bloom. This differs to the natural environment where a phytoplankton bloom can substantially modify (increase) pH. It also differs to the earlier mesocosms experiments that the authors reference in their discussion. I suggest that the authors discuss implications of the differences in the set-up of experiments.

Author's response to general comments: We thank the reviewer for the thorough evaluation of the manuscript and the insightful comments. The comment on our experimental approach is very appropriate and, as suggested, a new paragraph was added where its implications are discussed (see below). The experimental protocol where pH and pCO₂ are kept constant during the full experiment is indeed different to what would happen in nature where changes in photosynthesis and respiration during the bloom development would affect these parameters. The main reason why these conditions were kept constant was to allow us to precisely measure and maximise inference of the effects of pH and pCO₂ on different processes (e.g. phytoplankton photosynthesis in this paper, and dimethylsulfide production in a companion paper to be submitted) taking place during all phases of the bloom.

The following section has been added in the new version of the manuscript:

4.5: Implications and limitations

During our study, we chose to keep the pH constant during the whole experiment instead of allowing it to vary with changes in photosynthesis and respiration during the bloom phases. This approach differs from previous mesocosm experiments where generally no subsequent CO₂ manipulations are conducted after the initial targets are attained (Schulz et al. 2017 and therein). Keeping the pH and pCO₂ conditions stable during our study allowed us to precisely quantify the effect of the changing pH/pCO₂ on the processes taking place during the different phases of the bloom. Such control was not exercised in two of our mesocosms (i.e. the drifters). In these two mesocosms, the pH increased from 7.9 to 8.3 at 10°C, and from 7.9 to 8.7 at 15°C. Since the buffer capacity of acidified waters diminishes with increasing CO₂, the drift in pCO₂ and pH due to biological activity would have been even greater in the more acidified treatments (Delille et al., 2005; Riebesell et al., 2007). Hence, allowing the pH to drift in all mesocosms would have likely ended in an overlapping of the treatments where acidification effects would have been harder to detect. Thus, our experiment could be considered as an intermediate between strictly controlled small scale laboratory experiments and large scale pelagic mesocosm experiments in which only the initial conditions are set. By limiting pCO₂ decrease under high CO₂ drawdown due to photosynthesis during the bloom phase, we minimise confounding effects of

pCO₂ potentially overlapping in association with high biological activity in the mesocosms. Hence, the experimental conditions could be considered as extreme examples of acidification conditions, due to the extent of pCO₂ values studied. However, the absence of OA effects on most biological parameters measured during our study, even under these extreme conditions, strengthens the argument that the phytoplankton community in LSLE is resistant to OA.

Referee comment: Nutrient concentration and irradiance are main factors controlling phytoplankton growth in seawater. The authors should assess how these factors may have affected cell growth and primary production. This includes: 1. Add a drawing of the set-up and placement of mesocosms and treatments within the container. Containers often bear the risk of self-shading, which would need to be considered.

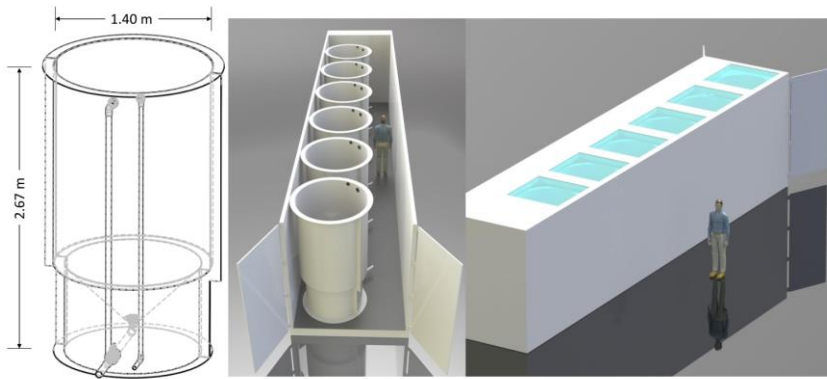
Author's response: We thank the reviewer for pointing that out. Light is indeed an important driver of phytoplankton photosynthesis and growth. As requested, the following information has been added in the text as well as a new figure:

Modification (line 88)

Old sentence: Each enclosure is sealed with a Plexiglas cover allowing the transmission of 90 % of photosynthetically active radiation (PAR; 400–700 nm), 50–85 % of solar UVB (280–315 nm) and 85–90 % of UVA (315–400 nm).

New sentence: The mesocosms exhibit opaque walls and all lie on the same plane level as not to shade each other. Light penetrates the mesocosms only through a sealed Plexiglas circular cover at their uppermost part. The cover allows the transmission of 90 % of photosynthetically active radiation (PAR; 400–700 nm), 85–90 % of UVA (315–400 nm), and 50–85 % of solar UVB (280–315 nm).

New figure (A):



In terms of the impact of nutrient concentrations on cell growth and primary production, we discuss this further: please refer to the specific comment about line 211 below.

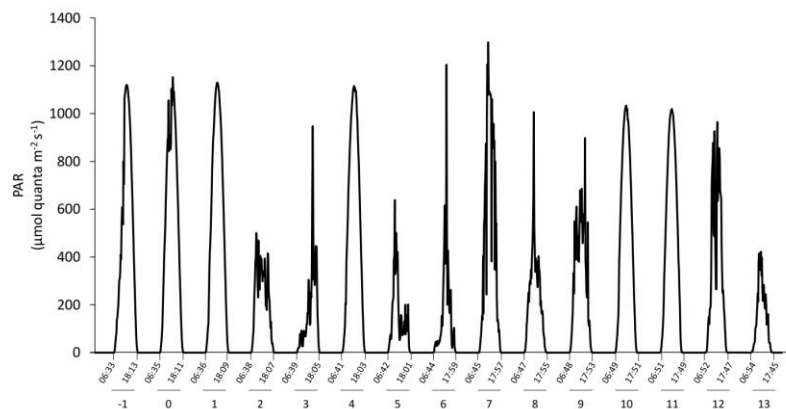
Referee comment: Please give absolute values for irradiance instead of % shading. What was the light:dark cycle? Since primary production measurements were carried out over 24h, some incubation hours will have been in the dark if natural sunlight was applied. It is important to inform about the potential role of dark respiration during the incubations. Since light intensity has been shown to co-affect phytoplankton responses to acidification and warming, it is absolutely necessary to show and discuss the light climate in mesocosms and incubations.

Author's response:

We acknowledge that light intensity has the potential to affect phytoplankton response to acidification and warming. Light intensity varied between days over the duration of the experiment (see new figure below). We cannot exclude the possible interaction of light intensity with acidification or warming, or the effect the varying intensity has on the dynamics of primary production. However, as all mesocosms were subjected to the same fluctuating natural irradiance, and that pCO_2 and temperature were the only factors changing between the treatments, we limited our interpretation to these two parameters.

New sentence (line 112): Incident light was variable during our experiment, with only few sunny days (Fig. B).

New figure (B):



Referee comment: It is important to consider that net primary production was measured. Hence, responses to warming and acidification may not only be related to photosynthetic production but also to respiration processes. Please discuss.

Author's response:

We agree with the reviewer. The text was modified accordingly (Line 394).

Old sentence: The warming-induced decrease in carbon fixation measured during Phase II may thus result from an increase in respiration by the nitrogen-limited diatoms.

New sentence: The warming-induced increase in fixed carbon being release in the dissolved fraction likely stems from increased exudation by phytoplankton, or sloppy feeding / excretion following ingestion by grazers (Kim et al., 2011). The increase in fixed carbon released as dissolved organic carbon (DOC) measured during Phase II may also result from greater respiration by the nitrogen-limited diatoms during periods of darkness of the incubations, as dark phytoplankton respiration rates generally increase with temperature (Butrón et al., 2009; Robarts and Zohary, 1987). Moreover, the enclosures do not permit the sinking and export of particulates organic carbon (POC), allowing a further transformation into DOC by heterotrophic bacteria, a process that could be exacerbated under warming (Wohlers et al., 2009).

Referee comment: Given that the authors did not add nutrients to the natural seawater, the strong increase in biomass (from 10 to up to 30 µg/L Chl a in one day) after incubation is very surprising. What could have limited phytoplankton growth in situ? Please discuss.

Author's response:

The following phrases were added to address this phenomenon (line 302).

New sentence: In situ nutrient conditions prior to the water collection were favourable for a bloom development. Based on previous studies, in situ phytoplankton growth was probably limited by light due to water turbidity and vertical mixing at the time of water collection (Levasseur et al. 1984). Grazing may also have played a role in keeping the in situ biomass of flagellates low prior to our sampling. However, a natural diatom fall bloom was observed in the days following the water collection in the adjacent region (Ferreyra, pers. comm.). The increased stability within the mesocosms, combined with the reduction of the grazing pressure (filtration on 250 µm) likely contributed to the fast accumulation of phytoplankton biomass.

Referee comment: There was a strong drop in pH prior to the acidification treatment on day -3. What may have been the reason for this drop?

Author's response (AR):

The following modifications have been made to address the pH drop / pCO₂ rise at the onset of the experiment.

Modification (line 200)

Old sentence: The pH remained relatively stable throughout the experiment in the pH-controlled treatments, but decreased slightly during Phase II by an average of -0.14 ± 0.07 units relative to the target pH_T (Fig. 1a).

New sentence: Following the filling of the mesocosms, the pH_T in all mesocosms decreased from an average of 7.84 to 7.53. Throughout the rest of the experiment after treatments were applied, the pH remained relatively stable in the pH-controlled treatments, but decreased slightly during Phase II by an average of -0.14 ± 0.07 units relative to the target pH_T (Fig. 1a).

Addition (line 294)

New sentence: The onset of the experiment was marked by an increase of pCO₂ on the day following the filling of the mesocosms. This phenomenon often takes place at the beginning of such experiments when pumping tends to break phytoplankton cells and larger debris into smaller ones. We attribute the rapid fluctuations in pCO₂ to the release of organic matter following the filling of the mesocosms with a stimulating effect on heterotrophic respiration, and hence CO₂ production.

Specific comments:

136
137 Line 87: add diameter and height of mesocosms
138 AR: Line 87 has been modified as follow: (note that the dimensions of the mesocosms are now also presented in the new
139 figure A):
140
141 Old sentence: The mesocosms are cylindrical with a cone-shaped bottom within which mixing is achieved using a propeller
142 fixed near the top.
143
144 New sentence: The mesocosms are cylindrical (2.67 m × 1.40 m) with a cone-shaped bottom within which mixing is achieved
145 using a propeller fixed near the top.
146
147 Line 99ff: add total duration of the experiment to the description
148 AR: Line 100 has been modified as follow:
149
150 Old sentence:
151 The water was collected at 5 m depth near Rimouski harbour (48° 28' 39.9" N, 68° 31' 03.0" W) on the 27th of September 2014.
152 In situ conditions were: salinity = 26.52, temperature = 10 °C, nitrate (NO₃⁻) = 12.8 ± 0.6 µmol L⁻¹, silicic acid
153 (Si(OH)₄) = 16 ± 2 µmol L⁻¹, and soluble reactive phosphate (SRP) = 1.4 ± 0.3 µmol L⁻¹. The same day (indicated as day -5
154 hereafter), the water was filtered through a 250 µm mesh while simultaneously filling the 12 mesocosm tanks by gravity with
155 a custom made 'octopus' tubing system.
156
157 New sentence:
158 The water was collected at 5 m depth near Rimouski harbour (48° 28' 39.9" N, 68° 31' 03.0" W) on the 27th of September 2014
159 (indicated as day -5 hereafter), and the experiment lasted until the 15th of October 2014 (day 13). In situ conditions were:
160 salinity = 26.52, temperature = 10 °C, nitrate (NO₃⁻) = 12.8 ± 0.6 µmol L⁻¹, silicic acid (Si(OH)₄) = 16 ± 2 µmol L⁻¹, and
161 soluble reactive phosphate (SRP) = 1.4 ± 0.3 µmol L⁻¹. On day -5, the water was filtered through a 250 µm mesh while
162 simultaneously filling the 12 mesocosm tanks by gravity with a custom made 'octopus' tubing system.
163
164 Line 104: give value for initial pCO₂
165 AR: Line 104 has been modified as follow:
166 Old sentence: The initial in situ temperature of 10 °C was maintained in the twelve mesocosms for the first 24 h (day -4).
167
168 New sentence: The initial pCO₂ was 623 ± 7 µatm and the in situ temperature of 10 °C was maintained in the twelve
169 mesocosms for the first 24 h (day -4).

Line 113ff: Add total amount of volume sampled from the mesocosms each day

AR: The following was added to line 116: “Total amount of volume sampled every day was 24 L or less.”

Line 166: Was the no replicate incubation? Was the error within treatment assessed?

AR: There was no replication of incubations. The number of bottles to handle was already quite extensive and the maximum capacity of our incubators had been reached. We chose to adopt the strategy of an increased number of treatments (mesocosms), which, even with reduced replication, allows greater power to characterise the functional relationships between OA parameters and organism or ecosystem response (Riebesell et al. 2011 (Guide to Best Practices in Ocean Acidification)). However, we conducted independent measures of particulate P_p , dissolved P_p , as well as total P_p every day in all the mesocosms allowing us to verify that the fractions measured in particulate and dissolved P_p reliably added up to the total P_p .

Line 171: Give irradiance values

AR: The daily irradiances are now presented in Figure B.

Line 202: pCO_2 was $1340 \pm 150 \mu atm$ on day -3; why was the value so high?

AR: The pCO_2 doubled after the filling of the mesocosms most probably due to an increase in CO_2 production following the release of organic matter and the increase in heterotrophic respiration. We conclude that the filling of the mesocosms tends to break phytoplankton cells and larger debris into smaller ones, with a stimulating effect on bacteria. Refer to additions on lines 200 and 294.

Line 211:’ The three nutrients displayed a similar temporal depletion pattern following the development of the phytoplanktonic bloom.‘ I disagree the nutrients in the warm treatments were clearly reduced much faster.

AR: Right. We meant that the general pattern was similar between the three nutrients (nitrate, soluble reactive phosphate and silicic acid) within each of the mesocosms, however we agree that clarity could be added here. We rephrased this part of the results section:

Old sentence: The three nutrients displayed a similar temporal depletion pattern following the development of the phytoplanktonic bloom.

New sentences: Within individual mesocosms, concentrations of nitrate, silicic acid and soluble reactive phosphate displayed similar temporal patterns following the development of the phytoplankton bloom. Overall, nutrient depletion was reached within 5 days in all mesocosms at $10^\circ C$, exception made of the drifter which became nutrient-deplete by day 3. Nutrient depletion was reached slightly earlier within the $15^\circ C$ mesocosms, all of them displaying exhaustion within 3 days of the

experiment. Accordingly, bloom development and primary production within each mesocosm were eventually limited by the supply in nutrients, irrespective of the temperature or pH treatment.

Line 217: ‘Chl a concentrations were below $1 \mu\text{g L}^{-1}$ just after the filling of the mesocosms, and averaged $5.9 \pm 0.6 \mu\text{g L}^{-1}$ on day 0’. If Chl a increased that much regardless of treatment; light limitation or exclusion of zooplankton probably had a major influence of phytoplankton development and should be considered in more depth.

AR: Water for our experiments was collected near shore where turbidity is high in this part of the St. Lawrence Estuary. We thus attribute the rapid response observed at the beginning of our incubations to an increase in light availability. The presence of high nutrient levels in the water at the beginning of the experiment also suggests that light intensity in the upper mixed layer was too low to allow the development of the bloom near the dock where the water was collected. Please refer to modifications made for line 302.

Line 327: The citation of Bach et al 2017 is not accurate as that study didn’t determine carbon fixation

AR: The citation of Bach et al., 2017 has been removed.

Figure 3: Wasn’t the Chl a accumulation (day 0 to Chl a max) not much higher in the warm control?

AR: Figure 3 y-axis has been adjusted.

Figure 5 g, f: same axis labelling different figure. . .please check.

AR: Figure 5g, e, f labelling has been verified. Figure 5j, k, l label has been modified from “Chl a-normalized P_p ($\mu\text{mol C} (\mu\text{g Chl a})^{-1} \text{d}^{-1}$)” to: “Chl a-normalized P_D ($\mu\text{mol C} (\mu\text{g Chl a})^{-1} \text{d}^{-1}$)”.

Referee comments #2: The manuscript of B nard and collaborators reports on an experiment that has been conducted using indoor mesocosms (2.6 m³) to test for the effect of ocean acidification and warming on the development of a fall phytoplankton bloom in the Lower St. Lawrence Estuary. The experiment setup comprised 2 sets of 6 mesocosms installed in two temperature-controlled containers, that were filled with seawater sieved onto 250 microns. In one container, the water temperature was raised by 5 C compared to the mesocosms installed in the other container (10 vs. 15 C). A gradient approach (no replicates) has been considered for pCO₂/pH covering a range of pH from 7.2 to 8.6. The experiment lasted 13 days and covered the development of a bloom and its decline. Major conclusions of this study are that pCO₂ has no effect on all measured parameters and processes while increasing temperature led to a faster build-up of chlorophyll and higher particulate primary production rates. Overall, this is a very well written manuscript that deals with an important topic. The introduction is well documented and shows that while this topic is of great importance, a fair amount of studies has already been conducted, including studies using in situ mesocosms in various environments. Although I would like to ultimately recommend this manuscript for publication in BG, I am concerned by 3 major aspects of this work and would like the authors to answer these comments.

Author’s response: We would like to thank the reviewer for the general evaluation of the manuscript and the insightful comments. We will further discuss the following comments of the reviewer.

Referee comment: Realism. The authors clearly mention that the surface mixed-layer pCO₂ is strongly modulated by biological productivity, yet they decided to run an experiment during which a bloom is produced and where carbonate chemistry has been maintained as constant. This would be acceptable if well explained and discussed, but the problem is that “control” mesocosms were actually not controlled (consider changing their name. . .) and pH was left increasing while the bloom was forming to (what I consider to be) very high and potentially unrealistic pH (?) values of 8.6. In situ pH was apparently close to 7.8, these “control” mesocosms appear to me as “perturbed”! Besides this major concern, I have to admit I do not understand how carbonate chemistry was controlled. The authors mention that “acidification” was carried out over day -1. On that day, I actually also observe a sudden increase of pH for the “controls”, pH8 and pH7.8. . . How did that happen? Naturally? Why was the increase in pH much higher in the controls than for the other mesocosms. Obviously, some information is missing here. Do you know the reason why pH decreased so fast between day -4 and day -3?

Author’s response: First, following this comment, the “Controls” have been more appropriately renamed “Drifters” to clearly show that the pCO₂ was not controlled. We noted that Reviewer #1 also pointed out the shortcomings in the discussion of the different approaches to control pH during this type of experiment.

The following section has been added in the new version of the manuscript:

4.5: Implications and limitations

During our study, we chose to keep the pH constant during the whole experiment instead of allowing it to vary with changes in photosynthesis and respiration during the bloom phases. This approach differs from previous mesocosm experiments where generally no subsequent CO₂ manipulations are conducted after the initial targets are attained (Schulz et al. 2017 and therein). Keeping the pH and pCO₂ conditions stable during our study allowed us to precisely quantify the effect of the changing pH/pCO₂ on the processes taking place during the different phases of the bloom. Such control was not exercised in two of our mesocosms (i.e. the drifters). In these two mesocosms, the pH increased from 7.9 to 8.3 at 10°C, and from 7.9 to 8.7 at 15°C. Since the buffer capacity of acidified waters diminishes with increasing CO₂, the drift in pCO₂ and pH due to biological activity would have been even greater in the more acidified treatments (Delille et al., 2005; Riebesell et al., 2007). Hence, allowing the pH to drift in all mesocosms would have likely ended in an overlapping of the treatments where acidification effects would have been harder to detect. Thus, our experiment could be considered as an intermediate between strictly controlled small scale laboratory experiments and large scale pelagic mesocosm experiments in which only the initial conditions are set. By limiting pCO₂ decrease under high CO₂ drawdown due to photosynthesis during the bloom phase, we minimise confounding effects of pCO₂ potentially overlapping in association with high biological activity in the mesocosms. Hence, the experimental conditions could be considered as extreme examples of acidification conditions, due to the extent of pCO₂ values studied. However, the absence of OA effects on the biological parameters measured during our study, even under these extreme conditions, strengthens the argument that the phytoplankton community in LSLE is resistant to OA.

To further clarify how the acidification and pH treatments were applied, the following has been added.

Addition (line 112):

To attain initial targeted pH, CO₂-saturated artificial seawater was added to the mesocosms that needed a pH lowering while mesocosms M2 (8.0), M4 (7.8), M6 (Drifter), M9 (8.0), M11 (Drifter) and M12 (7.8) were openly mixed to allow the degassing of the supersaturated CO₂. Once the mesocosms had reached their target pH, the automatic system controlled the sporadic addition of CO₂-saturated water to refrain the pH from rising. Only the “Drifters” were not controlled throughout the experiment.

Referee comment: Timing. The second concern I have is related to the division of the experiment in 2 phases. Phase 1 corresponds to the development of the diatom bloom extended up to the depletion of nitrate (day 0 to 4) and Phase 2 corresponds to the declining phase of the bloom in the absence of detectable nitrate. Except that this is not really true since temperature increased the speed at which chl_a built-up and nutrients were consumed (this is not really mentioned in 3.2). At 15°C, except for 1 mesocosm, nitrate was exhausted already on day 2 while at 10°C, NO₃ in most mesocosms were actually exhausted on day 4. My point is that since T modified the timing of the bloom (and its decline), it does not seem correct to me to consider fixed periods. The build-up of chl_a and all related statistical analyses should be conducted at 15°C between day 0 and 2, and all tests related to the decline of the bloom between day 3 and 13. Would that change some of your results?

Author's response:

We agree with the reviewer on the need for a better representation of the different phases in relation to the treatments but would previously like to inform on our decision to initially choose a fixed period. Firstly, it is imperative to divide the experiment in two phases not to confound effects caused by different processes and conditions during the development or the decline of the bloom. We previously considered multiple division method for the experiment (day of nitrate exhaustion, maximum Chl *a* concentration, averaged day of nitrate exhaustion) and ultimately opted for the averaged day of nitrate exhaustion as to mark the end of the nutrient-rich development phase. By choosing a single day as the divider for the phases, we could accurately compare our results with numerous mesocosms experiment that also divide their experiment using fixed periods. However, in many of those cases, the distinction between the phases were sharply defined as timing was not an important factor.

Thus, we agree with the reviewer suggestion but would like to take it one step further. Assigning phases duration based on temperature treatments as the reviewer suggests (Phase I: days 0-4 at 10°C, and days 0-2 at 15°C) would exclude some data from mesocosms that are still in the growth phase from the analyses of that phase, as M3 and M5 maximum Chl *a* concentrations are attained on day 7, and M7 maximum Chl *a* concentration is on day 4. Therefore, we suggest modifying the phases for each mesocosm as follow: Phase I (day 0 to day of maximum Chl *a* concentration) and Phase II (day after maximum Chl *a* concentration to day 13). By doing so, all the analyses on the Phase I will be constrained to the Chl *a* accumulation phase for each mesocosm, while Phase II will be an accurate representation of the individual declining phase. This modification carries some changes in the significance of the results of the analyses, although it does not change the overall narrative or conclusion of the manuscript. Namely, the absence of acidification effects is still valid for all parameters measured, except for picocyanobacteria abundance at 15°C during Phase II which is shows a negative linear trend with increasing pCO₂. We already suggested that increases in grazing pressures could counteract the stimulating effect of increased CO₂ availability on picocyanobacteria, and this is still valid. With regards to the temperature effects, the differences on the mean concentrations of Chl *a* is not significant in either phases. Although, the accumulation rate of Chl *a* is still higher at 15°C, reflecting the faster accumulation of Chl *a*. The temperature effects on particulate primary production during the both phases have also been discarded, yet our conclusion remains that the P_p is not affected over the full duration of the experiment. This will strengthen the conclusion that only the timing of the bloom development is affected by temperature, with negligible effects on the other parameters.

Moreover, we had already processed data in this manner and final figures can easily be produced to reflect the changes in the statistical analyses.

Referee comment: Grazing. I regret that potentially the most exciting result of this experiment suggesting that pCO₂ “positive” effects on phytoplankton were actually masked by significant increases in micro-grazing is not more developed. I understand the politics behind the publication of papers from a joint experiment, it would just bring much more value to your

paper if these results were incorporated and discussed. Top-down control is very often neglected in these OA-OW experiments.

Author's response:

We agree with this comment. The impact of the different treatments on zooplankton abundance will be discussed in a companion paper by colleagues.

Minor comments

L217: concentrations were

AR: "Concentrations where" changed to "concentrations were"

L225: "suggesting a faster loss of pigments. . .". Not really convinced by that. . . Is the slope different?

AR: Following the changes made with regards to the statistical analyses, this section was adjusted.

Old section (line 223-226):

During Phase II, we observed no significant effect of increasing pCO₂ on the mean Chl *a* concentrations at the two temperatures tested. Nevertheless, during that phase, the mean Chl *a* concentrations decreased from 18.2 ± 0.9 µg L⁻¹ at 10 °C to 12.4 ± 0.7 µg L⁻¹ at 15 °C, suggesting a faster loss of the pigments following the depletion of NO₃⁻.

New sentence:

During Phase II, we observed no significant effect of pCO₂, temperature, and the interaction of those factors on the mean Chl *a* concentrations following the depletion of NO₃⁻.

L230: "The strong correlation" I do not understand this sentence. How a correlation can suggest anything about importance?

AR: The sentence has been modified.

New sentence:

The correlation between the nanophytoplankton abundance and Chl *a* ($r^2 = 0.75$, $p < 0.001$, $df = 166$) suggests that this phytoplankton size class was responsible for most of the biomass build-up throughout the experiment.

Figure 1a: label pHT in situ, why in situ?

363 **AR:** All pH_T are measured at 25°C and are computed to the temperatures of the mesocosms. The label “ pH_T in situ” meant
364 that the pH_T is calculated at the in situ temperature of each mesocosm. Therefore, for mesocosms M1–M6 the pH_T is computed
365 at 10°C, while for mesocosms M7–M12 the pH_T is computed at 15°C. To avoid confusion, we changed the label to “ pH_T ”.
366

Experimental assessment of the sensitivity of an estuarine phytoplankton fall bloom to acidification and warming

Robin Bénard¹, Maurice Levasseur¹, Michael Grant Scarratt², Marie-Amélie Blais¹, Alfonso Mucci³, Gustavo Ferreyra⁴, Michel Starr², Michel Gosselin⁴, Jean-Éric Tremblay¹, Martine Lizotte¹

¹Département de biologie, Université Laval, 1045 avenue de la Médecine, Québec, Québec G1V 0A6, Canada

²Fisheries and Oceans Canada, Maurice Lamontagne Institute, P.O. Box 1000, Mont-Joli, Québec G5H 3Z4, Canada

³Department of Earth and Planetary Sciences, McGill University, 3450 University Street, Montréal, Québec H3A 2A7, Canada

⁴Institut des sciences de la mer de Rimouski (ISMER), Université du Québec à Rimouski, 310 allée des Ursulines, Rimouski, Québec G5L 3A1, Canada

Correspondence: Robin Bénard (robin.benard.1@ulaval.ca)

Field Code Changed

Abstract. We investigated the combined effect of ocean acidification and warming on the dynamics of the phytoplankton fall bloom in the Lower St. Lawrence Estuary (LSLE), Canada. Twelve 2600 L mesocosms were set to initially cover a wide range of pH_T (pH on the total proton scale) from 8.0 to 7.2 corresponding to a range of pCO₂ from 440 to 2900 µatm, and two temperatures (in situ and +5 °C). The 13-day experiment captured the development and decline of a nanophytoplankton bloom dominated by the chain-forming diatom *Skeletonema costatum*. During the development phase of the bloom, increasing pCO₂ influenced neither the magnitude nor the net growth rate of the nanophytoplankton bloom whereas increasing the temperature by 5 °C stimulated the chlorophyll *a* (Chl *a*) growth rate and maximal particulate primary production (P_P) by 7650 % and 63460 %, respectively. During the declining phase of the bloom, warming accelerated the loss of diatom cells, and paralleled by a gradual decrease in the abundance of photosynthetic picoeukaryotes and a bloom of picocyanobacteria. Increasing pCO₂ and warming did not influence the abundance of picoeukaryotes while picocyanobacteria abundance was reduced by the increase in pCO₂ when combined with warming in the latter phase of the experiment. negatively-affected P_P. Due to the countervailing responses of the plankton community to warming during the two phases of the experiment. Over the full duration of the experiment, the time-integrated net primary production was not significantly affected by the pCO₂ treatments or warming over the full duration of the study. The diatom bloom was paralleled by a gradual decrease in the abundance of photosynthetic picoeukaryotes and followed by a bloom of picocyanobacteria. Increasing pCO₂ and warming did not influence the abundance of picoeukaryotes, but warming stimulated picocyanobacteria proliferation. Overall, our results suggest that warming, rather than acidification, is more likely to alter phytoplankton autumnal bloom development in the LSLE in the decades to come. Future studies examining a broader gradient of temperatures should be conducted over a larger seasonal window in order to better constrain the potential effect of warming on the development of blooms in the LSLE and its impact on the fate of primary production.

397 **1. Introduction**

398 Anthropogenic emissions have increased atmospheric carbon dioxide (CO₂) concentrations from their pre-industrial value of
399 280 to 412 ppm in 2017, and concentrations of 850–1370 ppm are expected by the end of the century under the business-as-
400 usual scenario RCP 8.5 (IPCC, 2013). The global ocean has already absorbed about 28 % of these anthropogenic CO₂
401 emissions (Le Quéré et al., 2015), leading to a global pH decrease of 0.11 units (Gattuso et al., 2015), a phenomenon known
402 as Ocean Acidification (OA). The surface ocean pH is expected to decrease by an additional 0.3–0.4 units under the RCP 8.5
403 scenario by 2100, and as much as 0.8 units by 2300 (Caldeira and Wickett, 2005; Doney et al., 2009; Feely et al., 2009). The
404 accumulation of anthropogenic CO₂ in the atmosphere also results in an increase in the Earth's heat content that is primarily
405 absorbed by the ocean (Wijffels et al., 2016), leading to an expected rise of sea surface temperatures of 3 to 5 °C by 2100
406 (IPCC, 2013). Whereas the effect of increasing atmospheric CO₂ partial pressures (pCO₂) on ocean chemistry is relatively well
407 documented, the potential impacts of OA on marine organisms and how their response to OA will be modulated by the
408 concurrent warming of the ocean surface waters are still the subject of much debate (Boyd and Hutchins, 2012; Gattuso et al.,
409 2013).

410 Over the last decade, there has been increasing interest in the potential effects of OA on marine organisms (Kroeker et al.,
411 2013). The first experiments were primarily conducted on single phytoplankton species (reviewed in Riebesell and Tortell,
412 2011), but subsequent mesocosm experiments highlighted the impact of OA on the structure and productivity of complex
413 plankton assemblages (Riebesell et al., 2007, 2013). Due to their widely different initial and experimental conditions, these
414 ecosystem-level experiments generated contrasting results (Schulz et al., 2017) but some general patterns nevertheless
415 emerged. For example, diatoms generally benefit from higher pCO₂ through stimulated photosynthesis and growth rates since
416 the increase in CO₂ concentrations compensates for the low affinity of RubisCO towards CO₂ (Giordano et al., 2005; Gao and
417 Campbell, 2014). Although most phytoplankton species have developed carbon concentration mechanisms (CCM) to
418 compensate for the low affinity of RubisCO towards CO₂, CCM efficiencies differ between taxa, rendering predictions of the
419 impact of a CO₂ rise on the downregulation of CCM rather difficult (Raven et al., 2014). For example, some studies
420 unexpectedly reported no significant or very modest stimulation of primary production under elevated CO₂ concentrations
421 (Engel et al., 2005; Eberlein et al., 2017). OA can ultimately affect the structure of phytoplankton assemblages. Small cells
422 such as photosynthetic picoeukaryotes can benefit directly from an increase in pCO₂ as CO₂ can passively diffuse through their
423 boundary layer (Beardall et al., 2014), and the smallest organisms within this group could benefit most from the increase
424 (Brussaard et al., 2013). Accordingly, OA experiments have typically favoured smaller phytoplankton cells (Yoshimura et al.,
425 2010; Brussaard et al., 2013; Morán et al., 2015), although the proliferation of larger cells has also been reported (Tortell et
426 al., 2002). Hence, generic predictions of phytoplankton community responses to OA are challenging.

427 Few recent studies have investigated the combined effects of OA and warming on natural phytoplankton assemblages (Hare
428 et al., 2007; Feng et al., 2009; Maudgendre et al., 2015; Paul et al., 2015, 2016). Laboratory experiments have shown that OA
429 and warming could together increase photosynthetic rates, but at the expense of species richness, the reduction of diversity

predominantly imputable to warming (Tatters et al., 2013). Results of an experiment conducted with a natural planktonic community from the Mediterranean Sea showed no effect of a combined warming and decrease in pH on primary production, but higher picocyanobacteria abundances were observed in the warmer treatment (Maugendre et al., 2015). Shipboard microcosm incubations conducted in the northern South China Sea displayed higher phytoplankton biomass, daytime primary productivity and dark community respiration under warmer conditions, but these positive responses were cancelled at low pH (Gao et al., 2017). In contrast, a mesocosm experiment carried out with a fall planktonic community from the western Baltic Sea led to a decrease in phytoplankton biomass under warming, but combined warming and increased pCO₂ led to an increase in biomass (Sommer et al., 2015). Results from experiments where the impacts of pCO₂ and temperature are investigated individually may be misleading as multiple stressors can interact antagonistically or synergistically, sometimes in a nonlinear, unpredictable fashion (Todgham and Stillman, 2013; Boyd et al., 2015; Riebesell and Gattuso, 2015; Gunderson et al., 2016). The Lower St. Lawrence Estuary (LSLE) is a large (9350 km²) segment of the greater St. Lawrence Estuary (d'Anglejan, 1990). From June to September, the LSLE is characterized by a dynamic succession in the phytoplankton community, mostly driven by changes in light and nutrient availability through variations in the intensity of vertical mixing (Levasseur et al., 1984). The spring and fall blooms are mostly comprised of diatoms, with simultaneous nitrate and silicic acid exhaustion ultimately limiting primary production (Levasseur et al., 1987; Roy et al., 1996). How OA and warming may affect these blooms and primary production has never been investigated in the LSLE. The OA problem is complex in estuarine and coastal waters where freshwater runoff, tidal mixing, and high biological activity contribute to variations in pCO₂ and pH on different time scales (Duarte et al., 2013). The surface mixed-layer pCO₂ in the LSLE varies spatially from 139 to 548 µatm and is strongly modulated by biological productivity (Dinauer and Mucci, 2017). Surface pH_T has been shown to vary from 7.85 to 7.93 in a single tidal cycle in the LSLE, nearly as much as the world's oceans have experienced in response to anthropogenic CO₂ uptake over the last century (Caldeira and Wickett, 2005; Mucci et al., 2017).

The main objective of this study was to experimentally assess the sensitivity of the LSLE phytoplankton fall assemblage to a large pCO₂ gradient at two temperatures (in situ and +5 °C). Whether lower trophic-level microorganisms thriving in a highly variable environment will show higher resistance or resilience to future anthropogenic forcings is still a matter of speculation.

2. Material and methods

2.1 Mesocosm setup

The mesocosm system consists of two thermostated full-size ship containers each holding six 2600 L mesocosms (Aquabiotek Inc., Québec, Canada[®]). The mesocosms are cylindrical (2.67 m × 1.40 m) with a cone-shaped bottom within which mixing is achieved using a propeller fixed near the top (Fig. 1). ~~The mesocosms exhibit opaque walls and all lie on the same plane level as not to shade each other. Light penetrates the mesocosms only through a sealed Plexiglas circular cover at their uppermost part. The cover allows the transmission of 90 % of photosynthetically active radiation (PAR; 400–700 nm), 85–90 % of UVA (315–400 nm), and 50–85 % of solar UVB (280–315 nm). Each enclosure is sealed with a Plexiglas cover allowing the~~

transmission of 90 % of photosynthetically active radiation (PAR; 400–700 nm), 50–85 % of solar UVB (280–315 nm) and 85–90 % of UVA (315–400 nm). The mesocosms are equipped with individual, independent temperature probes (AQBT-Temperature sensor, accuracy ± 0.2 °C). Temperature in the mesocosms was measured every 15 minutes during the experiment, and the control system triggered either a resistance heater (Process Technology TTA1.8215) located near the middle of the mesocosm or a pump-activated glycol refrigeration system to maintain the set temperature. The pH in each mesocosm was monitored every 15 minutes using Hach® PD1P1 probes (± 0.02 pH units) connected to Hach® SC200 controllers, and positive deviations from the target values activated peristaltic pumps linked to a reservoir of artificial seawater equilibrated with pure CO₂ prior to the onset of the experiment. This system maintained the pH of the seawater in the mesocosms within ± 0.02 pH units of the targeted values by lowering the pH during autotrophic growth but could not increase the pH during bloom senescence when the pCO₂ rose and pH decreased.

2.2 Setting

The water was collected at 5 m depth near Rimouski harbour (48° 28' 39.9" N, 68° 31' 03.0" W) on the 27th of September 2014 (indicated as day -5 hereafter), and the experiment lasted until the 15th of October 2014 (day 13). In situ conditions were: salinity = 26.52, temperature = 10 °C, nitrate (NO₃⁻) = 12.8 ± 0.6 μmol L⁻¹, silicic acid (Si(OH)₄) = 16 ± 2 μmol L⁻¹, and soluble reactive phosphate (SRP) = 1.4 ± 0.3 μmol L⁻¹. On day -5, the water was filtered through a 250 μm mesh while simultaneously filling the 12 mesocosm tanks by gravity with a custom made 'octopus' tubing system. The water was collected at 5 m depth near Rimouski harbour (48° 28' 39.9" N, 68° 31' 03.0" W) on the 27th of September 2014. In situ conditions were: salinity = 26.52, temperature = 10 °C, nitrate (NO₃⁻) = 12.8 ± 0.6 μmol L⁻¹, silicic acid (Si(OH)₄) = 16 ± 2 μmol L⁻¹, and soluble reactive phosphate (SRP) = 1.4 ± 0.3 μmol L⁻¹. The same day (indicated as day -5 hereafter), the water was filtered through a 250 μm mesh while simultaneously filling the 12 mesocosm tanks by gravity with a custom made 'octopus' tubing system. The initial pCO₂ was 623 ± 7 μatm and the in situ temperature of 10 °C was maintained in the twelve mesocosms for the first 24 h (day -4). The initial in situ temperature of 10 °C was maintained in the twelve mesocosms for the first 24 h (day -4). After that period, the six mesocosms in one container were maintained at 10 °C while temperature was gradually increased to 15 °C during over day -3 in the six mesocosms of the other container. To avoid subjecting the planktonic communities to excessive stress due to sudden changes in temperature and pH while setting the experiment, the mesocosms were left to acclimatize on day -2 before acidification was carried out over day -1. One mesocosm from each temperature-controlled container was not pH-controlled to assess the community response to the freely fluctuating pH. These two mesocosms were labelled "Controls Drifters" as the initial in situ pH was allowed to fluctuate over time with the development of the phytoplankton bloom. The other mesocosms were set to cover a range of pH_T of ~~ea~~-8.0 to ~~ea~~-7.2 corresponding to a pCO₂ gradient of ~~ea~~-440 to ~~ea~~-2900 μatm after acidification was carried out. To attain initial targeted pH, CO₂-saturated artificial seawater was added to the mesocosms that needed a pH lowering while mesocosms M2 (8.0), M4 (7.8), M6 (Drifter), M9 (8.0), M11 (Drifter) and M12 (7.8) were openly mixed to allow the degassing of the supersaturated CO₂. Once the mesocosms had reached their target pH, the automatic system controlled the sporadic addition of CO₂-saturated water to refrain the pH

495 from rising. Only the Drifters were not controlled throughout the experiment. Incident light was variable during our
496 experiment, with only few sunny days (Fig. 2).

498 2.3 Seawater analysis

499 The mesocosms were sampled between 05:00 and 08:00 a.m. every day. Seawater for carbonate chemistry, nutrients, and
500 primary production were collected directly from the mesocosms as close to sunrise as possible. Seawater was also collected in
501 20 L carboys for the determination of chlorophyll *a* (Chl *a*), taxonomy, and other variables. Total amount of volume sampled
502 every day was 24 L or less. Samples for salinity were taken from the artificial seawater tanks and in the mesocosms on day -
503 3, 3 and 13. The samples were collected in 250 mL plastic bottles and stored in the dark until analysis was performed using a
504 Guildline Autosol 8400B Salinometer during the following months.

505 2.3.1 Carbonate chemistry

506 Carbonate chemistry parameters were determined using methods described in Mucci et al. (2017). Briefly, water samples for
507 pH (every day) and total alkalinity (TA, every 3–4 days) measurements were, respectively, transferred from the mesocosms to
508 125 mL plastic bottles without headspace and 250 mL glass bottles. A few crystals of HgCl₂ were added to the glass bottles
509 before sealing them with a ground-glass stopper and Apiezon® Type-M high-vacuum grease. The pH was determined within
510 hours of collection, after thermal equilibration at 25.0 ± 0.1 °C, using a Hewlett-Packard UV-Visible diode array
511 spectrophotometer (HP-8453A) and a 5 cm quartz cell with phenol red (PR; Robert-Baldo et al., 1985) and *m*-cresol purple
512 (mCP; Clayton and Byrne, 1993) as indicators. Measurements were carried out at the wavelength of maximum absorbance of
513 the protonated (HL) and deprotonated (L) indicators. Comparable measurements were carried out using a TRIS buffer prepared
514 at a practical salinity of ~~ea~~-25 before and after each set of daily measurements (Millero, 1986).

515 The pH on the total proton concentration scale (pH_T) of the buffer solutions and samples at 25 °C was calculated according to
516 the equation of Byrne (1987), using the salinity of each sample and the HSO₄⁻ association constants given by Dickson (1990).
517 The TA was determined on site within one day of sampling by open-cell automated potentiometric titration (Titrilab 865,
518 Radiometer®) with a pH combination electrode (pHC2001, Red Rod®) and a dilute (0.025N) HCl titrant solution. The titrant
519 was calibrated using Certified Reference Materials (CRM Batch#94, provided by A. G. Dickson, Scripps Institute of
520 Oceanography, La Jolla, USA). The average relative error, based on the average relative standard deviation on replicate
521 standard and sample analyses, was better than 0.15 %. The carbonate chemistry parameters at in situ temperature were then
522 calculated using the computed pH_T at 25 °C in combination with the measured TA using CO₂SYS (Pierrot et al., 2006) and
523 the carbonic acid dissociation constants of Cai and Wang (1998).

524 **2.3.3 Nutrients**

525 Samples for NO₃⁻, Si(OH)₄, and SRP analyses were collected directly from the mesocosms every day, filtered through
526 Whatman GF/F filters and stored at -20 °C in acid washed polyethylene tubes until analysis by a Bran and Luebbe Autoanalyzer
527 III using the colorimetric methods described by Hansen and Koroleff (2007). The analytical detection limit was 0.03-μmol L⁻¹
528 ¹ for NO₃⁻ plus nitrite (NO₂⁻), 0.02-μmol L⁻¹ for NO₂⁻, 0.1-μmol L⁻¹ for Si(OH)₄, and 0.05-μmol L⁻¹ for SRP.

529 **2.3.4 Plankton biomass, composition and enumeration**

530 Duplicate subsamples (100 mL) for Chl *a* determination were filtered onto Whatman GF/F filters. Chl *a* concentrations were
531 measured using a 10-AU Turner Designs fluorometer, following a 24 h extraction in 90 % acetone at 4 °C in the dark without
532 grinding (acidification method: Parsons et al., 1984). The analytical detection limit for Chl-*a* was 0.05 μg L⁻¹.
533 Pico- (0.2–2 μm) and nanophytoplankton (2–20 μm) cell abundances were determined daily by flow cytometry. Sterile
534 cryogenic polypropylene vials were filled with 4.95 mL of seawater to which 50 μL of glutaraldehyde Grade I (final
535 concentration = 0.1 %, Sigma Aldrich; Marie et al., 2005) were added. Duplicate samples were flash frozen in liquid nitrogen
536 after standing 15 minutes at room temperature in the dark. These samples were then stored at -80 °C until analysis. After
537 thawing to ambient temperature, samples were analyzed using a FACS Calibur flow cytometer (Becton Dickinson) equipped
538 with a 488 nm argon laser. The abundances of nanophytoplankton and picophytoplankton, which includes photosynthetic
539 picoeukaryotes and picocyanobacteria, were determined by their autofluorescence characteristics and size (Marie et al., 2005).
540 The biomass accumulation and nanophytoplankton growth rates were calculated by the following equation:

541
$$\mu = \ln(N_2/N_1) / (t_2 - t_1), \quad \text{_____} (1)$$

542 where N₁ and N₂ are the biomass or cell concentrations at given times t₁ and t₂, respectively.

543 Microscopic identification and enumeration for eukaryotic cells larger than 2 μm was conducted on samples taken from each
544 mesocosm on three days: day -4, the day when maximum Chl *a* was attained in each mesocosm, and day 13. Samples of
545 250 mL were collected and preserved with acidic Lugol solution (Parsons et al., 1984), then stored in the dark until analysis.
546 Cell identification was carried out at the lowest possible taxonomic rank using an inverted microscope (Zeiss Axiovert 10) in
547 accordance with Lund et al. (1958). The main taxonomic references used to identify the phytoplankton were Tomas (1997)
548 and Bérard-Therriault et al. (1999).

549 **2.3.5 Primary production**

550 Primary production was determined daily using the ¹⁴C-fixation incubation method (Knap et al., 1996; Ferland et al., 2011).
551 One clear and one dark 250 mL polycarbonate bottle were filled from each mesocosm at dawn and spiked with 250 μL of
552 NaH¹⁴CO₃ (80 μCi mL⁻¹). One hundred μL of 3-(3,4-dichlorophenyl)-1,1-dimethylurea (DCMU) (0.02 mol L⁻¹) was added to
553 the dark bottles to prevent active fixation of ¹⁴C by phytoplankton (Legendre et al., 1983). The total amount of radioisotope in
554 each bottle was determined by immediately pipetting 50 μL subsamples into a 20 mL scintillation vial containing 10 mL of

scintillation cocktail (Ecolume™) and 50 µL of ethanolamine (Sigma). Bottles were placed in separate incubators, at either 10 °C or 15 °C, under reduced (30 %) natural light for 24 h, which corresponds to the light transmittance at mid-mesocosm depth.

At the end of the incubation periods, 3 mL were transferred to a scintillation vial for determination of the total primary production (P_T), 3 mL were filtered through a syringe filter (GD/X 0.7 µm) to estimate daily photosynthetic carbon fixation released in the dissolved organic carbon pool (P_D). The remaining volume was filtered onto a Whatman GF/F filter to measure the particulate primary production (P_P). Vials containing the P_T and P_D samples were acidified with 500 µL of HCl 6 N, allowed to sit for 3 h under a fume hood, then neutralized with 500 µL of NaOH 6 N. The vials containing the filters were acidified with 100 µL of 0.05 N HCl and left to fume for 12 h. Fifteen mL of scintillation cocktail were added to the vials and they were stored pending analysis using a Tri-Carb 4910TR liquid scintillation counter (PerkinElmer). Rates of carbon fixation into particulate and dissolved organic matter were calculated according to Knap et al. (1996) using the dissolved inorganic carbon concentration computed for each mesocosm at the beginning of the daily incubations and multiplied by a factor of 1.05 to correct for the lower uptake of ^{14}C compared to ^{12}C .

2.4 Statistical analysis

All statistical analyses were performed using R (nlme package). A general least squares (gls) model approach was used to test the linear effects of the two treatments (temperature, pCO_2), and of their interactions on the measured variables (Paul et al., 2016; Husherr et al., 2017). The analysis was conducted independently on two different time periods: Phase I (day 0 to day of maximum Chl *a* concentration) was calculated individually for each mesocosm, whereas Phase II (day after maximum Chl *a* concentrations) corresponded to the declining phase of the bloom (Table 1).~~Phase I (day 0 to day 4) corresponded to the development of the diatom bloom and extended up to the depletion of nitrate, whereas Phase II (day 5 to day 13) corresponded to the declining phase of the bloom in the absence of detectable nitrate.~~ Averages (or time-integration in the case of primary production) of the response variables were calculated separately over the two phases and were plotted against pCO_2 . Separate regressions were performed with pCO_2 as the continuous factor for each temperature when a temperature effect or interaction with pCO_2 was detected in the gls model. Otherwise, the model included data from both temperatures and the interaction with pCO_2 . Normality of the residuals was determined using a Shapiro-Wilk test ($p > 0.05$) and data were transformed (natural logarithm or square root) if required. As explained by Havenhand et al. (2010), the gradient approach, instead of treatment replication, is particularly suitable when few experimental units are available such as in large volume mesocosm experiments. In addition, squared Pearson's correlation coefficients (r^2) with a significance level of 0.05 were used to evaluate correlations between key variables.

584 **3. Results**

585 **3.1 Seawater chemistry**

586 Water salinity was 26.52 ± 0.03 on day -4 in all mesocosms and remained constant throughout the experiment, averaging
587 26.54 ± 0.02 on day 13. The TA was practically invariant in the mesocosms, averaging $2057 \pm 2 \mu\text{mol kg}_{\text{sw}}^{-1}$ on day -4 and
588 $2058 \pm 2 \mu\text{mol kg}_{\text{sw}}^{-1}$ on day 13. Following the filling of the mesocosms, the pH_T in all mesocosms decreased from an average
589 of 7.84 to 7.53. Throughout the rest of the experiment after treatments were applied, the pH remained relatively stable in the
590 pH-controlled treatments, but decreased slightly during Phase II by an average of -0.14 ± 0.07 units relative to the target pH_T
591 (Fig. 3a). The pH remained relatively stable throughout the experiment in the pH-controlled treatments, but decreased slightly
592 during Phase II by an average of -0.14 ± 0.07 units relative to the target pH_T (Fig. 1a). Given a constant TA, pH variations
593 were accompanied by variations in pCO_2 , from an average of $1340 \pm 150 \mu\text{atm}$ on day -3, and ranging from 564 to 2902 μatm
594 at 10 °C, and from 363 to 2884 μatm at 15 °C on day 0 following the acidification (Fig. 3+b; Table 1). The pH_T in the
595 DrifterControls (M6 and M11) increased from 7.896 and 7.862 on day 0 at 10 °C and 15 °C, respectively, to 8.307 and 8.554
596 on day 13, reflecting the balance between CO_2 uptake and metabolic CO_2 production over the duration of the experiment. On
597 the last day, pCO_2 in all mesocosms ranged from 186 to 3695 μatm at 10 °C, and from 90 to 3480 μatm at 15 °C. The
598 temperature of the mesocosms in each container remained within ± 0.1 °C of the target temperature throughout the experiment
599 and averaged 10.04 ± 0.02 °C for mesocosms M1 through M6, and 15.0 ± 0.1 °C for mesocosms M7 through M12 (Fig. 3+c;
600 Table 1).

601 **3.2 Dissolved inorganic nutrient concentrations**

602 Nutrient concentrations averaged $9.1 \pm 0.5 \mu\text{mol L}^{-1}$ for NO_3^- , $13.4 \pm 0.3 \mu\text{mol L}^{-1}$ for Si(OH)_4 , and $0.91 \pm 0.03 \mu\text{mol L}^{-1}$ for
603 SRP on day 0 (Fig. 3+d, e, f). Within individual mesocosms, concentrations of nitrate, silicic acid and soluble reactive
604 phosphate displayed similar temporal patterns following the development of the phytoplankton bloom. Overall, NO_3^- depletion
605 was reached within 5 days in all mesocosms at 10 °C, exception made of the Drifter which became nutrient-deplete by day 3.
606 Nutrient depletion was reached slightly earlier within the 15 °C mesocosms, all of them displaying exhaustion within 3 days
607 of the experiment. Accordingly, bloom development and primary production within each mesocosm were eventually limited
608 by the supply in nutrients, irrespective of the temperature or pH treatment.The three nutrients displayed a similar temporal
609 depletion pattern following the development of the phytoplanktonic bloom. NO_3^- concentrations reached undetectable in all
610 mesocosms on day 5. Likewise, Si(OH)_4 fell below the detection limit between day 1 and 5 in all mesocosms except for those
611 whose pH_T was set at 7.2 and 7.6 at 10 °C (M5 and M3) and in which Si(OH)_4 depletion occurred on day 9. Variations in SRP
612 concentrations followed closely those of NO_3^- in all mesocosms except again for those set at pH 7.2 and 7.6 in which
613 undetectable values were reached on day 9.

3.3 Phytoplankton biomass

Chl *a* concentrations were below $1 \mu\text{g L}^{-1}$ just after the filling of the mesocosms, and averaged $5.9 \pm 0.6 \mu\text{g L}^{-1}$ on day 0 (Fig. 42a). They then quickly increased to reach maximum concentrations around $27 \pm 2 \mu\text{g L}^{-1}$ on day 3 \pm 2, and decreased progressively until the end of the experiment, reaching $11 \pm 1 \mu\text{g L}^{-1}$ and $2.4 \pm 0.2 \mu\text{g L}^{-1}$ at 10°C and 15°C on day 13. During Phase I, results from the gls model show no significant relationships between the mean Chl *a* concentrations and pCO_2 , temperature, and the interaction of the two factors at the two temperatures tested but significantly higher Chl *a* values at 15°C than at 10°C (Fig. 42b; Table 24). During this phase, the accumulation rate of Chl *a* was positively affected by temperature, increasing by $\sim 76\%$, but was not affected by the pCO_2 gradient at either temperature (Fig. 53a; Table 32). The maximum Chl *a* concentrations reached during the bloom were not affected by the two treatments (Fig. 53b; Table 32). During Phase II, we observed no significant effect of increasing pCO_2 , temperature, and the interaction of those factors on the mean Chl *a* concentrations following the depletion of NO_3^- (Fig. 4c; Table 4) at the two temperatures tested. Nevertheless, during that phase, the mean Chl *a* concentrations decreased from $18.2 \pm 0.9 \mu\text{g L}^{-1}$ at 10°C to $12.4 \pm 0.7 \mu\text{g L}^{-1}$ at 15°C , suggesting a faster loss of the pigments following the depletion of NO_3^- .

3.4 Phytoplankton size-class

Nanophytoplankton abundance varied from $8 \pm 1 \times 10^6$ cells L^{-1} on day 0 to an average maximum of $36 \pm 10 \times 10^6$ cells L^{-1} at the peak of the bloom (Fig. 42d). At both temperatures, nanophytoplankton abundance increased until at least days 2 or 4 and decreased or remained stable thereafter. The strong correlation between the nanophytoplankton abundance and Chl *a* ($r^2 = 0.7582$, $p < 0.001$, $\text{df} = 166$) suggests that this phytoplankton size class was responsible for most of the biomass build-up in the mesocosms throughout the experiment. As observed for the mean Chl *a* concentration, the mean abundance of nanophytoplankton was not significantly affected by the pCO_2 gradient at the two temperatures investigated during Phase I, but showed higher values at 15°C ($26.3 \pm 3.2 \times 10^6$ cells L^{-1}) than at 10°C ($13.14 \pm 2.1 \times 10^6$ cells L^{-1}) (Fig. 42e; Table 24). Likewise, the growth rate of nanophytoplankton during Phase I was not influenced by the pCO_2 gradient at the two temperatures but was significantly higher in the warm treatment (Fig. 53c; Table 32). During Phase II, no relationship was found between the mean nanophytoplankton abundance and the pCO_2 gradient, at the two temperatures, and no the $\text{pCO}_2 \times$ temperature effect interaction was observed (Fig. 42f; Table 43).

Initial abundance of photosynthetic picoeukaryotes was $10 \pm 2 \times 10^6$ cells L^{-1} , accounting for more than 80 % of total plankton cells in the $0.2\text{--}20 \mu\text{m}$ size fraction. The abundance of this plankton size fraction decreased slightly through Phase I and their number remained relatively stable at $43.3 \pm 30.2 \times 10^6$ cells L^{-1} throughout Phase II (Fig. 42g). We found no relationship between the abundance of picoeukaryotes and the pCO_2 gradient at the two temperatures investigated during both Phases I and II, and no temperature effect was observed either (Fig. 42h, i; Tables 24 and 43).

Picocyanobacteria exhibited a different pattern than the nanophytoplankton and picoeukaryotes (Fig. 42j). Their abundance was initially low ($1.7 \pm 0.3 \times 10^6$ cells L^{-1} on day 0), remained relatively stable during Phase I, and increased rapidly during

Phase II, accounting for ~~ca.~~ 50 % of the total picophytoplankton cell counts toward the end of the experiment. During Phase I, the mean picocyanobacteria abundance was not influenced by the pCO₂ gradient ~~but was higher at 15 °C~~ $(1.4 \pm 0.2 \times 10^6 \text{ cells L}^{-1})$ ~~than at 10 °C~~ $(0.95 \pm 0.05 \times 10^6 \text{ cells L}^{-1})$ ~~or temperature~~ (Fig. 42k; Table 24). During Phase II, their mean picocyanobacteria abundance ~~was not significantly affected by pCO₂ at in situ temperature, remained higher at~~ However, mean picocyanobacteria were higher at 15 °C, with the pCO₂ gradient responsible for a ~33% reduction of picocyanobacteria abundance from the Drifter to the more acidified treatment $(4.5 \pm 0.3 \times 10^6 \text{ cells L}^{-1} \text{ vs. } 3.0 \pm 0.3 \times 10^6 \text{ cells L}^{-1})$ ~~than at 10 °C~~ $(2.6 \pm 0.1 \times 10^6 \text{ cells L}^{-1})$, and again no significant effect of pCO₂ was detected (Fig 42l; Table 43).

3.5 Phytoplankton taxonomy

The taxonomic composition of the planktonic assemblage larger than 2 µm was identical in all treatments at the beginning of the experiment, and was mainly composed of the cosmopolitan chain-forming centric diatom *Skeletonema costatum* (*S. costatum*) and the cryptophyte *Plagioselmis prolunga* var. *nordica* (Fig. 64). At the peak of the blooms (maximum Chl *a* concentrations), the species composition did not vary between the pCO₂ treatments and between the two temperatures tested. *S. costatum* was the dominant species in all mesocosms (70–90 % of the total number of eukaryotic cells), except for one mesocosm (M3, pH 7.6 at 10 °C) where a mixed dominance of *Chrysochromulina* spp. (a prymnesiophyte of 2–5 µm) and *S. costatum* was observed (Fig. 64a). *S. costatum* accounted for 80–90 % of the total eukaryotic cell counts in all mesocosms at the end of the experiment carried out at 10 °C. At 15 °C, the composition of the assemblage had shifted toward a dominance of unidentified flagellates and choanoflagellates (2–20 µm) in all mesocosms with these two groups accounting for 55–80 % of the total cell counts while diatoms showed signs of loss of viability as indicated by the presence of empty frustules (Fig. 64b).

3.6 Primary production

P_P increased in all mesocosms during Phase I of the experiment, in parallel with the increase in Chl *a* (Fig. 75a). P_P maxima were attained on days 3–4, except for the 15 °C DrifterControl (M11) where P_P peaked on day 1. We found no significant effect of the pCO₂ gradient, ~~temperature and the pCO₂ × temperature interaction~~ on the time-integrated P_p ~~at the two temperatures during both Phases I and II~~ (Fig. 75b, c; Tables 24 and 43), ~~but time-integrated P_p was higher at 15 °C than at 10 °C during Phase I and lower at 15 °C than at 10 °C during Phase II~~ (Tables 1 and 3). Similarly, ~~opposite responses to warming were observed~~ the absence of significant treatment effects remained when normalizing P_p per unit of Chl *a* (Fig. 75g, h, i). Initial Chl *a*-normalized P_p values were $3.3 \pm 0.5 \mu\text{mol C } (\mu\text{g Chl } a)^{-1} \text{ d}^{-1}$ and reached maxima between $3.7 \pm 0.3 \mu\text{mol C } (\mu\text{g Chl } a)^{-1} \text{ d}^{-1}$ and $5.76 \pm 0.67 \mu\text{mol C } (\mu\text{g Chl } a)^{-1} \text{ d}^{-1}$ at 10 °C and 15 °C, respectively. These values then decreased to $2.2 \pm 0.6 \mu\text{mol C } (\mu\text{g Chl } a)^{-1} \text{ d}^{-1}$ and $0.9 \pm 0.2 \mu\text{mol C } (\mu\text{g Chl } a)^{-1} \text{ d}^{-1}$ on the last day of the experiment ~~(Fig. 5g)~~. During Phase I, the mean Chl *a*-normalized P_p was ~~not significantly affected by the pCO₂ gradient or higher under~~ warming, ~~but~~ as observed for the mean Chl *a* concentrations and time-integrated P_p over that phase, ~~was not affected by the pCO₂ gradient~~ (Fig. 75h; Table 24). During Phase II, the ~~log of the~~ mean Chl *a*-normalized P_p ~~was not significantly affected by the pCO₂~~

gradient, the temperature, or the interaction of these factors decreased with increasing temperature, with values of $2.2 \pm 0.2 \mu\text{mol C} (\mu\text{g Chl } a)^{-1} \text{d}^{-1}$ and $1.6 \pm 0.1 \mu\text{mol C} (\mu\text{g Chl } a)^{-1} \text{d}^{-1}$ at 10°C and 15°C , respectively (Fig. 75i; Table 43). No significant effect of pCO_2 was detected.

P_D was low at the beginning of the experiment, averaging $1.5 \pm 0.4 \mu\text{mol C L}^{-1} \text{d}^{-1}$, increased progressively during Phase I to reach maximum values of up to $6.48 \mu\text{mol C L}^{-1} \text{d}^{-1}$ on-between days 4 and 58 at the beginning of Phase II, and decreased thereafter (Fig. 75d). Time-integrated P_D was not significantly affected neither by the pCO_2 gradient, the temperature, and the $\text{pCO}_2 \times \text{temperature}$ interaction at the two temperatures tested nor by temperature during the two pPhases (Fig. 75e, f; Tables 24 and 43). Chl *a*-normalized P_D was low on day 0, averaging $0.3 \pm 0.1 \mu\text{mol C} (\mu\text{g Chl } a)^{-1} \text{d}^{-1}$, reached maximum values of $1.04 \pm 0.5.2 \mu\text{mol C} (\mu\text{g Chl } a)^{-1} \text{d}^{-1}$ at the beginning of Phase II and $1.6 \pm 0.2 \mu\text{mol C} (\mu\text{g Chl } a)^{-1} \text{d}^{-1}$ at 10°C and 15°C , then and-respectively decreased to $0.173 \pm 0.405 \mu\text{mol C} (\mu\text{g Chl } a)^{-1} \text{d}^{-1}$ and $0.6 \pm 0.2 \mu\text{mol C} (\mu\text{g Chl } a)^{-1} \text{d}^{-1}$ by the end of the experiment (Fig. 75j). During Phases I, and II, the mean Chl *a*-normalized P_D was affected neither by the pCO_2 gradient, the temperature and pCO_2 gradient, nor by the interaction between those factors (Fig. 75k, l; Tables 24 and 3). During Phase II, the log of the mean Chl *a*-normalized P_D was not affected by pCO_2 at either temperature tested, but significantly increased with warming (Fig. 7l; Table 4).

Figure 6 shows the influence of the treatments on maximum P_P and P_D as well as on the time-integrated P_P and P_D over the full length of the experiment. We found no effect of the pCO_2 gradient on the maximum P_P values at the two temperatures tested, but warming increased the maximum P_P values from $66 \pm 13 \mu\text{mol C L}^{-1} \text{d}^{-1}$ to $126 \pm 8 \mu\text{mol C L}^{-1} \text{d}^{-1}$ (Fig. 86a; Table 54). The time-integrated P_P over the full duration of the experiment was not affected by the pCO_2 gradient or the increase in temperature (Fig. 86b; Table 54). The absence of temperature effect results from the countervailing responses in time-integrated P_P between Phases I and II. The maximum P_D values were significantly affected by the treatments (Fig. 86c; Table 54). Maximum P_D decreased with increasing pCO_2 at in situ temperature but warming cancelled this effect (antagonistic effect). Nevertheless, the time-integrated P_D over the whole experiment did not vary significantly between treatments, although a decreasing tendency with increasing pCO_2 at 10°C and an increasing tendency with warming can be seen in Fig. 86d (Table 54).

4. Discussion

4.1 General characteristics of the bloom

The onset of the experiment was marked by an increase of pCO_2 on the day following the filling of the mesocosms. This phenomenon often takes place at the beginning of such experiments when pumping tends to break phytoplankton cells and larger debris into smaller ones. We attribute the rapid fluctuations in pCO_2 to the release of organic matter following the filling of the mesocosms with a stimulating effect on heterotrophic respiration, and hence CO_2 production. Then, Aa phytoplankton bloom, numerically dominated by the centric diatom *S. costatum*, took place in all mesocosms, regardless of treatments (Fig.

64). *S. costatum* is a common phytoplankton species in the St. Lawrence Estuary and in coastal waters (Kim et al., 2004; Starr et al., 2004; Annane et al., 2015). The length of the experiment (13 days) allowed us to capture both the development and declining phases of the bloom. The exponential growth phases lasted 1–4 days depending on the treatments, but maximal Chl *a* concentrations were reached only after 7 days in two of the twelve mesocosms (Fig. 42a; Table 1). The suite of measurements and statistical tests conducted did not provide any clues as to the underlying causes for the lower rates of biomass accumulation measured in these two mesocosms. Since statistical analyses conducted with or without these two apparent outliers gave similar results, they were not excluded from the analyses.

In situ nutrient conditions prior to the water collection were favourable for a bloom development. Based on previous studies, in situ phytoplankton growth was probably limited by light due to water turbidity and vertical mixing at the time of water collection (Levasseur et al. 1984). Grazing may also have played a role in keeping the in situ biomass of flagellates low prior to our sampling. However, a natural diatom fall bloom was observed in the days following the water collection in the adjacent region (Ferreira, pers. comm.). The increased stability within the mesocosms, combined with the reduction of the grazing pressure (filtration on 250 µm) likely contributed to the fast accumulation of phytoplankton biomass. During the development phase of the bloom, the concentration of all three monitored nutrients decreased, with NO₃⁻ and Si(OH)₄ reaching undetectable values. This nutrient co-depletion is consistent with results from previous studies suggesting a co-limitation of diatom blooms by these two nutrients in the St. Lawrence Estuary (Levasseur et al., 1987, 1990). Variations in P_P roughly followed changes in Chl *a*, and, as expected, the maximum Chl *a*-normalized P_P ($5 \pm 2 \mu\text{mol C} (\mu\text{g Chl } a)^{-1} \text{d}^{-1}$) was reached during the exponential growth phase in all mesocosms. Decreases in total phytoplankton abundances and P_P followed the bloom peaks and the timing of the NO₃⁻ and Si(OH)₄ depletions. A clear succession in phytoplankton size classes characterized the experiment. Nanophytoplankton cells were initially present in low abundance and became more numerous as the *S. costatum* diatom bloom developed. The ~~strong~~ correlation ($r^2 = 0.83$, $p < 0.001$, $df=34$) between the abundance of nanophytoplankton and *S. costatum* enumeration suggests that this cell size class can be used as a proxy of *S. costatum* counts in all mesocosms throughout the experiment. Nanophytoplankton cells accounted for $79 \pm 7 \%$ of total counts of cells $< 20 \mu\text{m}$ on the day of the maximum Chl *a* concentration. Accordingly, nanophytoplankton exhibited the same temporal trend as Chl *a* concentrations. During Phase II, nanophytoplankton abundances remained roughly stable at in situ temperature but decreased at 15 °C towards the end of the experiment. Photosynthetic picoeukaryotes were originally abundant and decreased throughout the experiment whereas picocyanobacteria abundances increased during Phase II. This is a typical phytoplankton succession pattern for temperate systems where an initial diatom bloom growing essentially on allochthonous nitrate gives way to smaller species growing on regenerated forms of nitrogen (Taylor et al., 1993).

4.2 Phase I (Diatom bloom development)

Our results show no significant effect of increasing pCO₂/decreasing pH on the mean abundance and net accumulation rate of the diatom-dominated nanophytoplankton assemblage during the development of the bloom (Figs. 42e and 53c). These results suggest that *S. costatum*, the species accounting for most of the biomass accumulation during the bloom, neither benefited

from the higher pCO₂ nor was negatively impacted by the lowering of pH. Assuming that *S. costatum* was also responsible for most of the carbon fixation during the bloom development phase, the absence of effect on P_P and Chl *a*-normalized P_P following increases in pCO₂ brings additional support to our conclusion. *S. costatum* operates a highly efficient CCM, minimizing the potential benefits of thriving in high CO₂ waters (Trimbom et al., 2009). This may explain why the strain present in the LSLE did not benefit from the higher pCO₂ conditions. Likewise, a mesocosm experiment conducted in the coastal North Sea showed no significant effect of increasing pCO₂ on carbon fixation during the development of the spring diatom bloom (Bach et al., 2017; Eberlein et al., 2017).

In addition to the aforementioned insensitivity to increasing pCO₂, our results point towards a strong resistance of *S. costatum* to severe pH decline. During our study, surprisingly constant rates of Chl *a* accumulation and nanophytoplankton growth (Fig. 53a, c), as well as maximum P_P (Fig. 86a), were measured during the development phase of the bloom over a range of pH_T extending from 8.6 to 7.2 (Fig. 34a). In a recent effort to estimate the causes and amplitudes of short-term variations in pH_T in the LSLE, Mucci et al. (2017) showed that pH_T in surface waters was constrained within a range of 7.85 to 7.93 during a 50-h survey over two tidal cycles at the head of the Laurentian Channel. It is notable that even the upwelling of water from 100 m depth or of low-oxygen LSLE bottom water would not decrease pH_T beyond ~7.75 and ~7.62, respectively (Mucci et al., 2017 and references therein). Our results show that the phytoplankton assemblage responsible for the fall bloom may tolerate even greater pH_T excursions. In the LSLE, such conditions may arise when the contribution of the low pH_T (7.12) freshwaters of the Saguenay River to the LSLE surface waters is amplified during the spring freshet. However, considering that comparable studies conducted in different environments have reported negative effects of decreasing pH on diatom biomass accumulation (Hare et al., 2007; Hopkins et al., 2010; Schulz et al., 2013), it cannot be concluded that all diatom species thriving in the LSLE are insensitive to acidification.

In contrast to the pCO₂ treatment, warming affected the development of the bloom in several ways. Increasing temperature by 5 °C significantly increased the accumulation rate of Chl *a*, and the nanophytoplankton growth rate, as well as the time-integrated P_P and Chl *a*-normalized P_P during Phase I of the bloom. The positive effects of warming on the Chl *a*-normalized maximum P_P during the development phase of the bloom most likely reflect the sensitivity of photosynthesis to temperature (Sommer and Lengfellner, 2008; Kim et al., 2013). It could also be related to optimal growth temperatures, which are often higher than in situ temperatures in marine phytoplankton (Thomas et al., 2012; Boyd et al., 2013). In support of this hypothesis, previous studies have reported optimal growth temperatures of 20–25 °C for *S. costatum*, which is 5–10 °C higher than the warmer treatment investigated in our study (Suzuki and Takahashi, 1995; Montagnes and Franklin, 2001). Extrapolating results from a mesocosm experiment to the field is not straightforward, as little is known of the projected warming of the upper waters of the LSLE in the next decades. In the Gulf of St. Lawrence, positive temperature anomalies in surface waters have varied from 0.25 to 0.75 °C per decade between 1985 and 2013 (Larouche and Galbraith, 2016). In the LSLE, warming of surface waters will likely result from a complex interplay between heat transfer at the air-water interface and variations in vertical mixing and upwelling of the cold intermediate layer at the head of the Estuary (Galbraith et al., 2014). Considering current

uncertainties regarding future warming of the LSLE, studies should be conducted over a wider range of temperatures in order to better constrain the potential effect of warming on the development of the blooms in the LSLE. Picoeukaryotes showed a more or less gradual decrease in abundance during Phase I, and our results show that this decline was not influenced by the increases in pCO₂ (Fig. 42g, h; Table 24). Picoeukaryotes are expected to benefit from high pCO₂ conditions even more so than diatoms as CO₂ can passively diffuse through their relatively thin boundary layer precluding the necessity of a costly uptake mechanism such as a CCM (Schulz et al., 2013). This hypothesis has been supported by several studies showing a stimulating effect of pCO₂ on picoeukaryote growth (Bach et al., 2016; Hama et al., 2016; Schulz et al., 2017 and references therein). On the other hand, in nature, the abundance of picoeukaryotes generally results from a delicate balance between cell division rates and cell losses through microzooplankton grazing and viral attacks. The few experiments, including the current study, reporting the absence or a modest effect of increasing pCO₂ on the abundance of eukaryotic picoplankton attribute their observations to an increase in nano- and microzooplankton grazing (Rose et al., 2009; Neale et al., 2014). During our experiment, the biomass of microzooplankton increased with increasing pCO₂ by ca. 200–300 % at the two temperatures tested (Ferreira and Lemli, unpubl. data). Thus, it is possible that a positive effect of increasing pCO₂ and warming on picoeukaryote abundances might have been masked by higher picoeukaryote losses due to increased microzooplankton grazing.

4.3 Phase II (declining phase of the bloom)

The gradual decrease in nanophytoplankton abundances coincided with an increase in the abundance of picocyanobacteria (Fig. 42j). ~~Regardless of *At in situ* temperature, the picocyanobacteria abundance during Phase II was unaffected by the increase in pCO₂ over the full range investigated (Fig. 42l; Table 43). The lack of positive response of picocyanobacteria to elevated pCO₂ was somewhat surprising considering that they have less efficient CCMs than diatoms (Schulz et al., 2013). Accordingly, several studies have reported a stimulation of the net growth rate of picocyanobacteria under elevated pCO₂ in different environments (coastal Japan, Mediterranean Sea, and Raunefjorden in Norway) and under different nutrient regimes, i.e. bloom and post-bloom conditions (Hama et al., 2016; Sala et al., 2016; Schulz et al., 2017). Consistent with our observations, however, Law et al. (2012) and Lomas et al. (2012) studies have also shown observed no direct effect of elevated pCO₂ on the net growth of picocyanobacteria during studies conducted in the Subtropical North Atlantic and the South Pacific (Law et al., 2012; Lomas et al., 2012). In our study, picocyanobacteria abundance was even reduced when high CO₂ was combined with warming. Similar negative effects of CO₂ on picocyanobacteria (particularly *Synechococcus*) have also been observed under later stages of bloom development, i.e. nutrient depletion, either caused by competition or grazing (Paulino et al., 2008; Hopkins et al., 2010). A potential increase in grazing pressure, following the rise in heterotrophic nanoflagellates abundance (e.g. choanoflagellates; Fig. 64b) measured under high pCO₂ and warmer conditions, could explain the ostensible absence of stimulation/negative effect of increasing pCO₂ on picocyanobacteria by increasing pCO₂ abundance in our experiment.~~ Despite the absence of grazing measurements during our study, our results support the hypothesis that the potential

for increased picocyanobacteria population growth under elevated pCO₂ and temperature is partially dependent on different grazing pressures (Fu et al., 2007).

Neither warming, nor acidification; affected the net particulate carbon fixation during the declining phase of the bloom. In our study, the time-integrated P_p and Chl *a*-normalized P_p were not significantly affected by the increase in pCO₂ during Phase II at the two temperatures tested (Fig. 75; Table 43). This result is surprising since nitrogen-limited cells have been shown to be more sensitive to acidification, resulting in a reduction in carbon fixation rates due to higher respiration (Wu et al., 2010; Gao and Campbell, 2014; Raven et al., 2014). Although our measurements do not allow to discriminate between the contributions of the different phytoplankton size classes to carbon fixation, we can speculate that diatoms, which were still abundant during Phase II, contributed to a significant fraction of the primary production. If so, these results suggest that *S. costatum* remained insensitive to OA even under nutrient stress. However, in contrast to Phase I, increasing the temperature by 5 °C during Phase II significantly reduced P_p and increased the Chl *a*-normalized P_p . Dark phytoplankton respiration rates generally increase with temperature (Butrón et al., 2009; Robarts and Zohary, 1987). The warming-induced decrease in carbon fixation increase in fixed carbon being release in the dissolved fraction likely stems from increased exudation by phytoplankton, or sloppy feeding / excretion following ingestion by grazers (Kim et al., 2011). The increase in fixed carbon released as dissolved organic carbon (DOC) measured during Phase II may also result from greater respiration by the nitrogen-limited diatoms during periods of darkness of the incubations, as dark phytoplankton respiration rates generally increase with temperature (Butrón et al., 2009; Robarts and Zohary, 1987). Moreover, the enclosures do not permit the sinking and export of particulates organic carbon (POC), allowing a further transformation into DOC by heterotrophic bacteria, a process that could be exacerbated under warming (Wohlers et al., 2009) measured during Phase II may thus result from an increase in respiration by the nitrogen limited diatoms.

4.4 Effect of the treatments on primary production over the full experiment

As mentioned above, increasing pCO₂ had no effect on time-integrated P_p during the two phases of the bloom, and but warming resulted respectively in a positive and negative effect during Phases I and II. Only affected the maximum P_p . As a result, primary production rates integrated over the whole duration of the experiment were not significantly different between the two temperatures tested. Although not statistically significant, the time-integrated P_D s over the full experiment displays a slight decrease with increasing pCO₂ at 10 °C and overall higher values in the warmer treatment (Fig. 86d; Table 54). Previous studies have reported increases of dissolved organic carbon (DOC) exudation (Engel et al., 2013), but also decreasing DOC concentrations at elevated pCO₂ under nitrate limitation (Yoshimura et al., 2014). The increase in DOC exudation is attributed to a stimulation of photosynthesis resulting from its sensitivity to higher pCO₂ (Engel et al. 2013), but the causes for a decrease in DOC concentrations at high pCO₂ are less clear and potentially attributable to an increase in transparent exopolymer particle (TEP) production (Yoshimura et al, 2014). Elevated TEP production under high pCO₂ conditions has been measured both at the peak of a bloom in a mesocosm study (Engel et al., 2014), and in post-bloom nutrient depleted conditions (MacGilchrist et al., 2014). However, during our study, TEP production decreased under high pCO₂ (Gaaloul, 2017). Thus,

the apparent decrease in P_D cannot be attributed to a greater conversion of exuded dissolved carbohydrate into TEP. The apparent rise in P_D under warming is consistent with previous studies reporting similar increases in phytoplankton dissolved carbon release with temperature (Morán et al., 2006; Engel et al., 2011). Although these apparent changes in P_D with increasing pCO_2 and warming require further investigations, they suggest that a larger proportion (~ea. 15 % of P_T at 15 °C compared to 10 % at 10 °C) of the newly fixed carbon could be exuded and become available for heterotrophic organisms under warmer conditions.

4.5 Implications and limitations

During our study, we chose to keep the pH constant during the whole experiment instead of allowing it to vary with changes in photosynthesis and respiration during the bloom phases. This approach differs from previous mesocosm experiments where generally no subsequent CO_2 manipulations are conducted after the initial targets are attained (Schulz et al. 2017 and therein). Keeping the pH and pCO_2 conditions stable during our study allowed us to precisely quantify the effect of the changing pH/ pCO_2 on the processes taking place during the different phases of the bloom. Such control was not exercised in two of our mesocosms (i.e. the Drifters). In these two mesocosms, the pH_T increased from 7.9 to 8.3 at 10 °C, and from 7.9 to 8.7 at 15 °C. Since the buffer capacity of acidified waters diminishes with increasing CO_2 , the drift in pCO_2 and pH due to biological activity would have been even greater in the more acidified treatments (Delille et al., 2005; Riebesell et al., 2007). Hence, allowing the pH to drift in all mesocosms would have likely ended in an overlapping of the treatments where acidification effects would have been harder to detect. Thus, our experiment could be considered as an intermediate between strictly controlled small scale laboratory experiments and large scale pelagic mesocosm experiments in which only the initial conditions are set. By limiting pCO_2 decrease under high CO_2 drawdown due to photosynthesis during the development of the bloom phase, we minimise confounding effects of pCO_2 potentially overlapping in association with high biological activity in the mesocosms. Hence, the experimental conditions could be considered as extreme examples of acidification conditions, due to the extent of pCO_2 values studied. However, the absence of OA effects on most biological parameters measured during our study, even under these extreme conditions, strengthens the argument that the phytoplankton community in LSLE is resistant to OA.

5. Conclusion

Our results reveal a remarkable resistance of the different phytoplankton size classes to the large range of pCO_2 /pH investigated during our study. It is noteworthy that the plankton assemblage was submitted to decreases in pH far exceeding those that they are regularly exposed to in the LSLE. The resistance of *S. costatum* to the pCO_2 treatments suggests that the acidification of surface waters of the LSLE will not affect the development rate and the amplitude of fall blooms dominated by this species. Photosynthetic picoeukaryotes and picocyanobacteria thriving alongside the blooming diatoms were also insensitive to acidification. In contrast to the pCO_2 treatments, warming the water by 5 °C had multiple impacts on the development and decline of the bloom. The 5 °C warming hastened the development of the diatom bloom (albeit with no increase in total cells

number) and increased the abundance of picocyanobacteria during Phase II despite a reduction under high pCO₂. These temperature-induced variations in the phytoplankton assemblage were accompanied by an increase in maximal P_r and suggest a potential increase in P_D under warming, although no significant changes in time-integrated P_r and P_D were observed over the phases or the full temporal scale of the experiment, respectively, by higher then lower P_r during the development and declining phases of the diatom bloom. Due to these contrasting responses, warming had no net effect on P_r over the full temporal scale of the experiment. Overall, our results indicate that warming could have more important impacts than acidification on phytoplankton bloom development in the LSLE in the next decades. Future studies should be conducted and specifically designed to better constrain the potential effects of warming on phytoplankton succession and primary production in the LSLE.

Data availability. The data have been submitted to be freely accessible via <https://issues.pangaea.de/browse/PDI-16607>, or can be obtained by contacting the author (robin.benard.1@ulaval.ca).

Author contributions. R. Bénard was responsible for the experimental design elaboration, data sampling and processing, and the redaction of this article. Several co-authors supplied specific data included in this article, and all co-authors contributed to this final version of the article.

Competing interests. The authors declare that they have no conflict of interest.

Acknowledgements

The authors wish to thank the Station Aquicole ISMER, especially Nathalie Morin and her staff, for their support during the project. We also wish to acknowledge Gilles Desmeules, Bruno Cayouette, Sylvain Blondeau, Claire Lix, Rachel Husscherr, Liliane St-Amand, Marjolaine Blais, Armelle Simo and Sonia Michaud for their help in setting up, sampling and processing samples during the experiment. The authors want to thank Jean-Pierre Gattuso for his constructive comments on an earlier draft of this manuscript. This study was funded by a Team grant from the Fonds de la Recherche du Québec – Nature et Technologies (FRQNT-Équipe-165335), the Canada Foundation for Innovation, and the Canada Research Chair on Ocean Biogeochemistry and Climate. This is a contribution to the research programme of Québec-Océan.

References

- Annane, S., St-Amand, L., Starr, M., Pelletier, E., and Ferreyra, G. A.: Contribution of transparent exopolymeric particles (TEP) to estuarine particulate organic carbon pool, Mar. Ecol. Prog. Ser., 529, 17–34, doi:10.3354/meps11294, 2015.
- Bach, L. T., Taucher, J., Boxhammer, T., Ludwig, A., Aberle-Malzahn, N., Abrahamsson, K., Almén, A. K., Asplund, M. E., Audritz, S., Boersma, M., Breitbarth, E., Bridges, C., Brussaard, C., Brutemark, A., Clemmesen, C., Collins, S., Crawford, K., Dahlke, F., Deckelnick, M., Dittmar, T., Doose, R., Dupont, S., Eberlein, T., Endres, S., Engel, A., Engström-Öst, J., Febiri, S., Fleischer, D., Fritsche, P., Gledhill, M., Göttler, G., Granberg, M., Grossart, H. P., Grifos, A., Hoffmann, L., Karlsson, A., Klages, M., John, U., Jutfelt, F., Köster, I., Lange, J., Leo, E., Lischka, S., Lohbeck, K., Lundve, B., Mark, F. C., Meyerhöfer,

902 M., Nicolai, M., Pansch, C., Petersson, B., Reusch, T., De Moraes, K. R., Schartau, M., Scheinin, M., Schulz, K. G., Schwarz,
 903 U., Stenegren, M., Stiasny, M., Storch, D., Stühr, A., Sswat, L., Svensson, M., Thor, P., Voss, M., Van De Waal, D., Wannicke,
 904 N., Wohlrab, S., Wulff, A., Achterberg, E. P., Algueró-Muñiz, M., Anderson, L. G., Bellworthy, J., Büdenbender, J., Czerny,
 905 J., Ericson, Y., Esposito, M., Fischer, M., Haunost, M., Hellemann, D., Horn, H. G., Hornick, T., Meyer, J., Sswat, M., Zark,
 906 M., and Riebesell, U.: Influence of ocean acidification on a natural winter-to-summer plankton succession: First insights from
 907 a long-term mesocosm study draw attention to periods of low nutrient concentrations, *PLoS ONE*, 11(8), 1–33,
 908 doi:10.1371/journal.pone.0159068, 2016.

~~909 Bach, L. T., Alvarez-Fernandez, S., Hornick, T., Stühr, A., and Riebesell, U.: Simulated ocean acidification reveals winners
 910 and losers in coastal phytoplankton, *PLoS ONE*, 12(11), 1–22, doi:10.1371/journal.pone.0188198, 2017.~~

911 Beardall, J., Stojkovic, S., and Gao, K.: Interactive effects of nutrient supply and other environmental factors on the sensitivity
 912 of marine primary producers to ultraviolet radiation: Implications for the impacts of global change, *Aquat. Biol.*, 22, 5–23,
 913 doi:10.3354/ab00582, 2014.

914 Bérard-Therriault, L., Poulin, M., and Bossé, L.: Guide d'identification du phytoplancton marin de l'estuaire et du golfe du
 915 Saint-Laurent incluant également certains protozoaires., Canadian Special Publication of Fisheries and Aquatic Sciences, 128,
 916 1–387, doi :10.1139/9780660960579, 1999.

917 Boyd, P. W., and Hutchins, D. A.: Understanding the responses of ocean biota to a complex matrix of cumulative
 918 anthropogenic change, *Mar. Ecol. Prog. Ser.*, 470, 125–135, doi:10.3354/meps10121, 2012.

919 Boyd, P. W., Rynearson, T. A., Armstrong, E. A., Fu, F., Hayashi, K., Hu, Z., Hutchins, D. A., Kudela, R. M., Litchman, E.,
 920 Mulholland, M. R., Passow, U., Strzepek, R. F., Whittaker, K. A., Yu, E., and Thomas, M. K.: Marine Phytoplankton
 921 temperature versus growth responses from polar to tropical waters - outcome of a scientific community-wide study, *PLoS*
 922 *ONE*, 8(5), doi:10.1371/journal.pone.0063091, 2013.

923 Boyd, P. W., Lennartz, S. T., Glover, D. M., and Doney, S. C.: Biological ramifications of climate-change-mediated oceanic
 924 multi-stressors, *Nat. Clim. Chang.*, 5(1), 71–79, doi:10.1038/nclimate2441, 2015.

925 Brussaard, C. P. D., Noordeloos, A. A. M., Witte, H., Collenteur, M. C. J., Schulz, K., Ludwig, A., and Riebesell, U.: Arctic
 926 microbial community dynamics influenced by elevated CO₂ levels, *Biogeosciences*, 10(2), 719–731, doi:10.5194/bg-10-719-
 927 2013, 2013.

928 Butrón, A., Iriarte, A., and Madariaga, I.: Size-fractionated phytoplankton biomass, primary production and respiration in the
 929 Nervión-Ibaizabal estuary: A comparison with other nearshore coastal and estuarine ecosystems from the Bay of Biscay, *Cont.*
 930 *Shelf Res.*, 29(8), 1088–1102, doi:10.1016/j.csr.2008.11.013, 2009.

931 Byrne, R. H.: Standardization of Standard Buffers by Visible Spectrometry, *Anal. Chem.*, 59, 1479–1481,
 932 doi:10.1021/ac00137a025, 1987.

933 Cai, W. J., and Wang, Y.: The chemistry, fluxes, and sources of carbon dioxide in the estuarine waters of the Satilla and
 934 Altamaha Rivers, Georgia, *Limnol. Oceanogr.*, 43(4), 657–668, doi:10.4319/lo.1998.43.4.0657, 1998.

Caldeira, K., and Wickett, M. E.: Ocean model predictions of chemistry changes from carbon dioxide emissions to the atmosphere and ocean, *J. Geophys. Res.*, 110(C9), 1–12, doi:10.1029/2004JC002671, 2005.

Clayton, T. D., and Byrne, R. H.: Spectrophotometric seawater pH measurements: total hydrogen ion concentration scale calibration of m-cresol purple and at-sea results, *Deep. Res. Part I*, 40(10), 2115–2129, doi:10.1016/0967-0637(93)90048-8, 1993.

d'Anglejan, B.: Recent sediments and sediment transport processes in the St. Lawrence Estuary, in: *Oceanography of a large-scale estuarine system*, Eds: El-Sabh, M. I., and Silverberg, N., Springer-Verlag, New York, USA, 109–129, doi:10.1002/9781118663783.ch6, 1990.

[Delille, B., Harlay, J., Zondervan, I., Jacquet, S., Chou, L., Wollast, R., Bellerby, R. G. J., Frankignoulle, M., Borges, A. V., Riebesell, U. and Gattuso, J. P.: Response of primary production and calcification to changes of pCO₂ during experimental blooms of the coccolithophorid *Emiliania huxleyi*, *Global Biogeochem. Cycles*, 19\(2\), 1–14, doi:10.1029/2004GB002318, 2005.](#)

Dickson, A. G.: Standard potential of the reaction: $\text{AgCl(s)} + 1/2\text{H}_2\text{(g)} = \text{Ag(s)} + \text{HCl(aq)}$ and the standard acidity constant of the ion HSO_4^- in synthetic sea water from 273.15 to 318.15 K, *J. Chem. Thermodyn.*, 22(2), 113–127, doi:10.1016/0021-9614(90)90074-Z, 1990.

Dinauer, A., and Mucci, A.: Spatial variability in surface-water pCO₂ and gas exchange in the world's largest semi-enclosed estuarine system: St. Lawrence Estuary (Canada), *Biogeosciences*, 14(13), 3221–3237, doi:10.5194/bg-14-3221-2017, 2017.

Doney, S. C., Fabry, V. J., Feely, R. A., and Kleypas, J. A.: Ocean acidification: The other CO₂ problem, *Ann. Rev. Mar. Sci.*, 1(1), 169–192, doi:10.1146/annurev.marine.010908.163834, 2009.

Duarte, C. M., Hendriks, I. E., Moore, T. S., Olsen, Y. S., Steckbauer, A., Ramajo, L., Carstensen, J., Trotter, J. A., and McCulloch, M.: Is ocean acidification an open-ocean syndrome? Understanding anthropogenic impacts on seawater pH, *Estuaries Coasts*, 36(2), 221–236, doi:10.1007/s12237-013-9594-3, 2013.

Eberlein, T., Wohlrab, S., Rost, B., John, U., Bach, L. T., Riebesell, U., and Van De Waal, D. B.: Effects of ocean acidification on primary production in a coastal North Sea phytoplankton community, *PLoS ONE*, 12(3), e0172594, doi:10.1371/journal.pone.0172594, 2017.

Engel, A., Zondervan, I., Aerts, K., Beaufort, L., Benthien, A., Chou, L., Delille, B., Gattuso, J.-P., Harlay, J., Heeman, C., Hoffmann, L., Jacquet, S., Nejstgaard, J., Pizay, M.-D., Rochelle-Newall, E., Schneider, U., Terbruggen A., and Riebesell, U.: Testing the direct effect of CO₂ concentration on a bloom of the coccolithophorid *Emiliania huxleyi* in mesocosm experiments, *Limnol. Oceanogr.*, 50(2), 493–507, doi:10.4319/lo.2005.50.2.0493, 2005.

Engel, A., Händel, N., Wohlers, J., Lunau, M., Grossart, H.-P., Sommer, U., and Riebesell, U.: Effects of sea surface warming on the production and composition of dissolved organic matter during phytoplankton blooms: Results from a mesocosm study, *J. Plankton Res.*, 33(3), 357–372, doi:10.1093/plankt/fbq122, 2011.

Engel, A., Borchard, C., Piontek, J., Schulz, K. G., Riebesell, U., and Bellerby, R.: CO₂ increases ¹⁴C primary production in an Arctic plankton community, *Biogeosciences*, 10(3), 1291–1308, doi:10.5194/bg-10-1291-2013, 2013.

Engel, A., Piontek, J., Grossart, H.-P., Riebesell, U., Schulz, K. G., and Sperling, M.: Impact of CO₂ enrichment on organic matter dynamics during nutrient induced coastal phytoplankton blooms, *J. Plankton Res.*, 36(3), 641–657, doi:10.1093/plankt/fbt125, 2014.

Feely, R. A., Doney, S. C., and Cooley, S. R.: Ocean acidification: present conditions and future changes in a high-CO₂ world, *Oceanography*, 22(4), 36–47, doi:10.5670/oceanog.2009.95, 2009.

Feng, Y., Hare, C. E., Leblanc, K., Rose, J. M., Zhang, Y., DiTullio, G. R., Lee, P. A., Wilhelm, S. W., Rowe, J. M., Sun, J., Nemcek, N., Gueguen, C., Passow, U., Benner, I., Brown, C., and Hutchins, D. A.: Effects of increased pCO₂ and temperature on the North Atlantic spring bloom. I. The phytoplankton community and biogeochemical response, *Mar. Ecol. Prog. Ser.*, 388, 13–25, doi:10.3354/meps08133, 2009.

Ferland, J., Gosselin, M., and Starr, M.: Environmental control of summer primary production in the Hudson Bay system: The role of stratification, *J. Mar. Syst.*, 88(3), 385–400, doi:10.1016/j.jmarsys.2011.03.015, 2011.

Gaaloul, H.: Effets du changement global sur les particules exopolymériques transparentes au sein de l'estuaire maritime du Saint-Laurent, M.Sc. thesis, Université du Québec à Rimouski, Canada, 133 pp., 2017.

Galbraith, P. S., Chassé, J., Gilbert, D., Larouche, P., Caverhill, C., Lefaiivre, D., Brickman, D., Pettigrew, B., Devine, L., and Lafleur, C.: Physical Oceanographic Conditions in the Gulf of St. Lawrence in 2013, DFO Can. Sci. Advis. Sec. Res. Doc., 2014/062(November), vi + 84 pp, 2014.

Gao, K., and Campbell, D. A.: Photophysiological responses of marine diatoms to elevated CO₂ and decreased pH: A review, *Funct. Plant Biol.*, 41(5), 449–459, doi:10.1071/FP13247, 2014.

Gao, G., Jin, P., Liu, N., Li, F., Tong, S., Hutchins, D. A., and Gao, K.: The acclimation process of phytoplankton biomass, carbon fixation and respiration to the combined effects of elevated temperature and pCO₂ in the northern South China Sea, *Mar. Pollut. Bull.*, 118(1–2), 213–220, doi:10.1016/j.marpolbul.2017.02.063, 2017.

Gattuso, J. P., Mach, K. J., and Morgan, G.: Ocean acidification and its impacts: An expert survey, *Clim. Change*, 117(4), 725–738, doi:10.1007/s10584-012-0591-5, 2013.

Gattuso, J.-P., Magnan, A., Bille, R., Cheung, W. W. L., Howes, E. L., Joos, F., Allemand, D., Bopp, L., Cooley, S. R., Eakin, C. M., Hoegh-Guldberg, O., Kelly, R. P., Portner, H.-O., Rogers, a. D., Baxter, J. M., Laffoley, D., Osborn, D., Rankovic, A., Rochette, J., Sumaila, U. R., Treyer, S., and Turley, C.: Contrasting futures for ocean and society from different anthropogenic CO₂ emissions scenarios, *Science*, 349(6243), doi:10.1126/science.aac4722, 2015.

Giordano, M., Beardall, J., and Raven, J. A.: CO₂ concentrating mechanisms in algae: Mechanisms, environmental modulation., and evolution, *Annu. Rev. Plant Biol.*, 56(1), 99–131, doi:10.1146/annurev.arplant.56.032604.144052, 2005.

Gunderson, A. R., Armstrong, E. J., and Stillman, J. H.: Multiple stressors in a changing World: The need for an improved perspective on physiological responses to the dynamic marine environment, *Ann. Rev. Mar. Sci.*, 8(1), 357–378, doi:10.1146/annurev-marine-122414-033953, 2016.

1001 Hama, T., Inoue, T., Suzuki, R., Kashiwazaki, H., Wada, S., Sasano, D., Kosugi, N., and Ishii, M.: Response of a phytoplankton
1002 community to nutrient addition under different CO₂ and pH conditions, *J. Oceanogr.*, 72(2), 207–223, doi:10.1007/s10872-
1003 015-0322-4, 2016.

1004 Hansen, H. P., and Koroleff, F.: Determination of nutrients, in: *Methods of Seawater Analysis*, 3, Eds: Grasshoff K., Kremling,
1005 K., and Ehrhardt, M., Wiley-VCH Verlag GmbH, Weinheim, Germany, 159–228, doi:10.1002/9783527613984.ch10, 2007.

1006 Hare, C. E., Leblanc, K., DiTullio, G. R., Kudela, R. M., Zhang, Y., Lee, P. A., Riseman, S., and Hutchins, D. A.: Consequences
1007 of increased temperature and CO₂ for phytoplankton community structure in the Bering Sea, *Mar. Ecol. Prog. Ser.*, 352, 9–16,
1008 doi:10.3354/meps07182, 2007.

1009 Havenhand, J., Dupont, S., and Quinn, G. P.: Designing ocean acidification experiments to maximise inference, in *Guide to*
1010 *best practices for ocean acidification research and data reporting*, Eds: Riebesell, U., Fabry, V. J., and Gattuso, J.-P.,
1011 Publications Office of the European Union, Luxembourg, 67–80, 2010.

1012 Hopkins, F. E., Turner, S. M., Nightingale, P. D., Steinke, M., Bakker, D., and Liss, P. S.: Ocean acidification and marine
1013 trace gas emissions, *Proc. Natl. Acad. Sci. U.S.A.*, 107(2), 760–765, doi:10.1073/pnas.0907163107, 2010.

1014 Husherr, R., Levasseur, M., Lizotte, M., Tremblay, J. É., Mol, J., Thomas, H., Gosselin, M., Starr, M., Miller, L. A., Jarníková,
1015 T., Schuback, N., and Mucci, A.: Impact of ocean acidification on Arctic phytoplankton blooms and dimethyl sulfide
1016 concentration under simulated ice-free and under-ice conditions, *Biogeosciences*, 14(9), 2407–2427, doi:10.5194/bg-14-2407-
1017 2017, 2017.

1018 IPCC: Working Group I Contribution to the Fifth Assessment Report Climate Change 2013: The Physical Science Basis,
1019 Intergov. Panel Clim. Chang., 1535, doi:10.1017/CBO9781107415324., 2013.

1020 Kim, K. Y., Garbary, D. J., and McLachlan, J. L.: Phytoplankton dynamics in Pomquet Harbour, Nova Scotia: a lagoon in the
1021 southern Gulf of St Lawrence, *Phycologica*, 43(3), 311–328, 2004.

1022 [Kim, J. M., Lee, K., Shin, K., Yang, E. J., Engel, A., Karl, D. M. and Kim, H. C.: Shifts in biogenic carbon flow from particulate](#)
1023 [to dissolved forms under high carbon dioxide and warm ocean conditions, *Geophys. Res. Lett.*, 38\(8\),](#)
1024 [doi:10.1029/2011GL047346, 2011.](#)

1025 Kim, J. H., Kim, K. Y., Kang, E. J., Lee, K., Kim, J. M., Park, K. T., Shin, K., Hyun, B., and Jeong, H. J.: Enhancement of
1026 photosynthetic carbon assimilation efficiency by phytoplankton in the future coastal ocean, *Biogeosciences*, 10(11), 7525–
1027 7535, doi:10.5194/bg-10-7525-2013, 2013.

1028 Knap, A., Michaels, A., Close, A. R., Ducklow, H., and Dickson, A. G.: Protocols for the Joint Global Ocean Flux Study
1029 (JGOFS) core measurements, JGOFS Rep No. 19, Reprint of the IOC Manuals and Guides No. 29, UNESCO, Bergen, Norway,
1030 doi:10013/epic.27912, 1996.

1031 Kroeker, K. J., Kordas, R. L., Crim, R., Hendriks, I. E., Ramajo, L., Singh, G. S., Duarte, C. M., and Gattuso, J. P.: Impacts of
1032 ocean acidification on marine organisms: Quantifying sensitivities and interaction with warming, *Glob. Chang. Biol.*, 19(6),
1033 1884–1896, doi:10.1111/gcb.12179, 2013.

1034 Larouche, P., and Galbraith, P. S.: Canadian coastal seas and Great Lakes sea surface temperature climatology and recent
1035 trends, *Can. J. Remote Sens.*, 42(3), 243–258, doi:10.1080/07038992.2016.1166041, 2016.

1036 Law, C. S., Breitbarth, E., Hoffmann, L. J., McGraw, C. M., Langlois, R. J., Laroche, J., Marriner, A., and Safi, K. A.: No
1037 stimulation of nitrogen fixation by non-filamentous diazotrophs under elevated CO₂ in the South Pacific, *Glob. Chang. Biol.*,
1038 18, 3004–3014, 2012.

1039 Le Quéré, C., Moriarty, R., Andrew, R. M., Canadell, J. G., Sitch, S., Korsbakken, J. I., Friedlingstein, P., Peters, G. P., andres,
1040 R. J., Boden, T. A., Houghton, R. A., House, J. I., Keeling, R. F., Tans, P., Arneeth, A., Bakker, D. C. E., Barbero, L., Bopp,
1041 L., Chang, J., Chevallier, F., Chini, L. P., Ciais, P., Fader, M., Feely, R. A., Gkritzalis, T., Harris, I., Hauck, J., Ilyina, T., Jain,
1042 A. K., Kato, E., Kitidis, V., Klein Goldewijk, K., Koven, C., Landschützer, P., Lauvset, S. K., Lefèvre, N., Lenton, A., Lima,
1043 I. D., Metzl, N., Millero, F., Munro, D. R., Murata, A., S. Nabel, J. E. M., Nakaoka, S., Nojiri, Y., O'Brien, K., Olsen, A.,
1044 Ono, T., Pérez, F. F., Pfeil, B., Pierrot, D., Poulter, B., Rehder, G., Rödenbeck, C., Saito, S., Schuster, U., Schwinger, J.,
1045 Séférian, R., Steinhoff, T., Stocker, B. D., Sutton, A. J., Takahashi, T., Tilbrook, B., Van Der Laan-Luijkx, I. T., Van Der
1046 Werf, G. R., Van Heuven, S., Vandemark, D., Viovy, N., Wiltshire, A., Zaehle, S., and Zeng, N.: Global Carbon Budget 2015,
1047 *Earth Syst. Sci. Data*, 7(2), 349–396, doi:10.5194/essd-7-349-2015, 2015.

1048 Legendre, L., Demers, S., Yentsch, C. M., and Yentsch, C. S.: The ¹⁴C method: Patterns of dark CO₂ fixation and DCMU
1049 correction to replace the dark bottle, *Limnol. Oceanogr.*, 28(5), 996–1003, doi:10.4319/lo.1983.28.5.0996, 1983.

1050 Levasseur, M., Theriault, J.-C., and Legendre, L.: Hierarchical control of phytoplankton succession by physical factors, *Mar.*
1051 *Ecol. Prog. Ser.*, 19, 211–222, doi:10.3354/meps019211, 1984.

1052 Levasseur, M. E., and Theriault, J.-C.: Phytoplankton biomass and nutrient dynamics in a tidally induced upwelling: the role
1053 of the NO₃:SiO₄ ratio, *Mar. Ecol. Prog. Ser.*, 39, 87–97, 1987.

1054 Levasseur, M. E., Harrison, P. J., Heimdahl, B. R., and Theriault, J.-C.: Simultaneous nitrogen and silicate deficiency of a
1055 phytoplankton community in a coastal jet-front, *Mar. Biol.*, 104(2), 329–338, doi:10.1007/BF01313275, 1990.

1056 Lomas, M. W., Hopkinson, B. M., Losh, J. L., Ryan, D. E., Shi, D. L., Xu, Y., and Morel, F. M. M.: Effect of ocean acidification
1057 on cyanobacteria in the subtropical North Atlantic, *Aquat. Microb. Ecol.*, 66(3), 211–222, doi:10.3354/ame01576, 2012.

1058 Lund, J. W. G., Kipling, C., and Le Cren, E. D.: The inverted microscope method of estimating algal numbers and the statistical
1059 basis of estimates by counting, *Hydrobiologia*, 11, 143–170, 1958.

1060 MacGilchrist, G. A., Shi, T., Tyrrell, T., Richier, S., Moore, C. M., Dumousseaud, C., and Achterberg, E. P.: Effect of enhanced
1061 pCO₂ levels on the production of dissolved organic carbon and transparent exopolymer particles in short-term bioassay
1062 experiments, *Biogeosciences*, 11(13), 3695–3706, doi:10.5194/bg-11-3695-2014, 2014.

1063 Marie, D., Simon, N., and Vaulot, D.: Phytoplankton cell counting by flow cytometry, *Algal Cult. Tech.*, 253–267,
1064 doi:10.1016/B978-012088426-1/50018-4, 2005.

1065 Maugendre, L., Gattuso, J. P., Louis, J., De Kluijver, A., Marro, S., Soetaert, K., and Gazeau, F.: Effect of ocean warming and
1066 acidification on a plankton community in the NW Mediterranean Sea, *ICES J. Mar. Sci.*, 72(6), 1744–1755,
1067 doi:10.1093/icesjms/fsu161, 2015.

1068 Millero, F. J.: The pH of estuarine waters, *Limnol. Oceanogr.*, 31(4), 839–847, doi:10.4319/lo.1986.31.4.0839, 1986.

1069 Montagnes, D. J. S., and Franklin, M.: Effect of temperature on diatom volume, growth rate, and carbon and nitrogen content:
1070 Reconsidering some paradigms, *Limnol. Oceanogr.*, 46(8), 2008–2018, doi:10.4319/lo.2001.46.8.2008, 2001.

1071 Morán, X. A. G., Sebastián, M., Pedrós-Alió, C., and Estrada, M.: Response of Southern Ocean phytoplankton and
1072 bacterioplankton production to short-term experimental warming, *Limnol. Oceanogr.*, 51(4), 1791–1800,
1073 doi:10.4319/lo.2006.51.4.1791, 2006.

1074 Morán, A. G., Alonso-sa, L., Nogueira, E., Ducklow, H. W., Gonza, N., Calvo-di, A., Arandia-gorostidi, N., Di, L., Huete-
1075 stauffer, T. M., Rey, U., and Carlos, J.: More, smaller bacteria in response to ocean's warming?, *Proc. R. Soc.*, 282(1810), 1–
1076 9, doi:http://dx.doi.org/10.1098/rspb.2015.0371, 2015.

1077 Mucci, A., Levasseur, M., Gratton, Y., Martias, C., Scarratt, M., Gilbert, D., Tremblay, J.-É., Ferreyra, G., and Lansard, B.:
1078 Tidally-induced variations of pH at the head of the Laurentian Channel, *Can. J. Fish. Aquat. Sci.*, doi:10.1139/cjfas-2017-
1079 0007, 2017.

1080 Neale, P. J., Sobrino, C., Segovia, M., Mercado, J. M., Leon, P., Cortés, M. D., Tuite, P., Picazo, A., Salles, S., Cabrerizo, M.
1081 J., Prasil, O., Montecino, V., and Reul, A.: Effect of CO₂, nutrients and light on coastal plankton. I. Abiotic conditions and
1082 biological responses, *Aquat. Biol.*, 22, 25–41, doi:10.3354/ab00587, 2014.

1083 Parsons, T. R., Maita, Y., and Lalli, C. M.: A manual of chemical and biological methods for seawater analysis, Pergamon
1084 Press, New York, 1984.

1085 Paul, C., Matthiessen, B., and Sommer, U.: Warming, but not enhanced CO₂ concentration, quantitatively and qualitatively
1086 affects phytoplankton biomass, *Mar. Ecol. Prog. Ser.*, 528, 39–51, doi:10.3354/meps11264, 2015.

1087 Paul, C., Sommer, U., Garzke, J., Moustaka-Gouni, M., Paul, A., and Matthiessen, B.: Effects of increased CO₂ concentration
1088 on nutrient limited coastal summer plankton depend on temperature, *Limnol. Oceanogr.*, 61(3), 853–868,
1089 doi:10.1002/lno.10256, 2016.

1090 [Paulino, A. I., Egge, J. K. and Larsen, A.: Effects of increased atmospheric CO₂ on small and intermediate sized osmotrophs](#)
1091 [during a nutrient induced phytoplankton bloom, *Biogeosciences*, 5\(3\), 739–748, doi:10.5194/bg-5-739-2008, 2008.](#)

1092 Pierrot, D., Lewis, E., and Wallace, D. W. R.: MS Excel program developed for CO₂ system calculations, Carbon Dioxide
1093 Information Analysis Center, ORNL/CDIAC-105a, Oak Ridge National Laboratory, US Department of Energy, Oak Ridge,
1094 592 Tennessee, 2006.

1095 Raven, J. A., Beardall, J., and Giordano, M.: Energy costs of carbon dioxide concentrating mechanisms in aquatic organisms,
1096 *Photosynth. Res.*, 121, 111–124, 2014.

1097 Riebesell, U., and Gattuso, J.-P.: Lessons learned from ocean acidification research, *Nat. Clim. Chang.*, 5(1), 12–14,
1098 doi:10.1038/nclimate2456, 2015.

1099 Riebesell, U., and Tortell, P. D.: Effects of ocean acidification on pelagic organism and ecosystems, in *Ocean Acidification*,
1100 Eds: Gattuso J.-P., and Hansson L., Oxford University Press, New York, 99–121, 2011.

1101 Riebesell, U., Schulz, K. G., Bellerby, R. G. J., Botros, M., Fritsche, P., Meyerhöfer, M., Neill, C., Nondal, G., Oschlies, a,
 1102 Wohlers, J., and Zöllner, E.: Enhanced biological carbon consumption in a high CO₂ ocean., *Nature*, 450(7169), 545–548,
 1103 doi:10.1038/nature06267, 2007.
 1104 Riebesell, U., Czerny, J., Von Bröckel, K., Boxhammer, T., Büdenbender, J., Deckelnick, M., Fischer, M., Hoffmann, D.,
 1105 Krug, S. A., Lentz, U., Ludwig, A., Muche, R., and Schulz, K. G.: Technical Note: A mobile sea-going mesocosm system -
 1106 New opportunities for ocean change research, *Biogeosciences*, 10(3), 1835–1847, doi:10.5194/bg-10-1835-2013, 2013.
 1107 Robarts, R. D., and Zohary, T.: Temperature effects on photosynthetic capacity, respiration., and growth rates of bloom-
 1108 forming cyanobacteria, *New Zeal. J. Mar. Freshw. Res.*, 21(3), 391–399, doi:10.1080/00288330.1987.9516235, 1987.
 1109 Robert-Baldo, G., Morris, M., and Byrne, R.: Spectrophotometric determination of seawater pH using phenol red, *Anal. Chem.*,
 1110 3(57), 2564–2567, doi:10.1021/ac00290a030, 1985.
 1111 Rose, J. M., Feng, Y., Gobler, C. J., Gutierrez, R., Harel, C. E., Leblanc, K., and Hutchins, D. A.: Effects of increased pCO₂
 1112 and temperature on the North Atlantic spring bloom. II. Microzooplankton abundance and grazing, *Mar. Ecol. Prog. Ser.*, 388,
 1113 27–40, doi:10.3354/meps08134, 2009.
 1114 Roy, S., Chanut, J.-P., Gosselin, M., and Sime-Ngando, T.: Characterization of phytoplankton communities in the Lower St.
 1115 Lawrence Estuary using HPLC-detected pigments and cell microscopy, *Mar. Ecol. Prog. Ser.*, 142, 55–73,
 1116 doi:10.3354/meps142055, 1996.
 1117 Sala, M. M., Aparicio, F. L., Balagué, V., Boras, J. A., Borrell, E., Cardelús, C., Cros, L., Gomes, A., López-Sanz, A., Malits,
 1118 A., Martínez, R. A., Mestre, M., Movilla, J., Sarmento, H., Vázquez-Domínguez, E., Vaqué, D., Pinhassi, J., Calbet, A., Calvo,
 1119 E., Gasol, J. M., Pelejero, C., and Marrasé, C.: Contrasting effects of ocean acidification on the microbial food web under
 1120 different trophic conditions, *ICES J. Mar. Sci.*, 73(3), 670–679, doi:10.1093/icesjms/fsv130, 2016.
 1121 Schulz, K. G., Bellerby, R. G. J., Brussaard, C. P. D., Büdenbender, J., Czerny, J., Engel, A., Fischer, M., Koch-Klavsén, S.,
 1122 Krug, S. A., Lischka, S., Ludwig, A., Meyerhöfer, M., Nondal, G., Silyakova, A., Stühr, A., and Riebesell, U.: Temporal
 1123 biomass dynamics of an Arctic plankton bloom in response to increasing levels of atmospheric carbon dioxide, *Biogeosciences*,
 1124 10(1), 161–180, doi:10.5194/bg-10-161-2013, 2013.
 1125 Schulz, K. G., Bach, L. T., Bellerby, R. G. J., Bermudez, R., Budenbender, J., Boxhammer, T., Czerny, J., Engel, A., Ludwig,
 1126 A., Meyerhofer, M., Larsen, A., Paul, A., Sswat, M., and Riebesell, U.: Phytoplankton blooms at increasing levels of
 1127 atmospheric carbon dioxide: experimental evidence for negative effects on prymnesiophytes and positive on small
 1128 picoeukaryotes, *Front. Mar. Sci.*, 4, 64, doi:10.3389/fmars.2017.00064, 2017.
 1129 Sommer, U., and Lengfellner, K.: Climate change and the timing, magnitude, and composition of the phytoplankton spring
 1130 bloom, *Glob. Chang. Biol.*, 14(6), 1199–1208, doi:10.1111/j.1365-2486.2008.01571.x, 2008.
 1131 Sommer, U., Paul, C., and Moustaka-Gouni, M.: Warming and ocean acidification effects on phytoplankton - From species
 1132 shifts to size shifts within species in a mesocosm experiment, *PLoS ONE*, 10(5), 17, doi:10.1371/journal.pone.0125239, 2015.
 1133 Starr, M., St-Amand, L., Devine, L., Bérard-Therriault, L., and Galbraith, P. S.: State of phytoplankton in the Estuary and Gulf
 1134 of St. Lawrence during 2003, *CSAS Res. Doc.*, 2004/123, 35, 2004.

Suzuki, Y., and Takahashi, M.: Growth responses of several diatom species isolated from various environments to temperature, *J. Phycol.*, 31(6), 880–888, doi:10.1111/j.0022-3646.1995.00880.x, 1995.

Tatters, A. O., Roleda, M. Y., Schnetzer, A., Fu, F., Hurd, C. L., Boyd, P. W., Caron, D. A., Lie, A. A. Y., Hoffmann, L. J., and Hutchins, D. A.: Short- and long-term conditioning of a temperate marine diatom community to acidification and warming, *Philos. Trans. R. Soc. Lond. B. Biol. Sci.*, 368(1627), 20120437, doi:10.1098/rstb.2012.0437, 2013.

Taylor, A. H., Harbour, D. S., Harris, R. P., Burkill, P. H., and Edwards, E. S.: Seasonal succession in the pelagic ecosystem of the North Atlantic and the utilization of nitrogen, *J. Plankton Res.*, 15(8), 875–891, doi:10.1093/plankt/15.8.875, 1993.

Thomas, M. K., Kremer, C. T., Klausmeier, C. a and Litchman, E.: A global pattern of thermal adaptation in marine phytoplankton., *Science*, 338(6110), 1085–1088, doi:10.1126/science.1224836, 2012.

Todgham, A. E., and Stillman, J. H.: Physiological responses to shifts in multiple environmental stressors: Relevance in a changing world, *Integr. Comp. Biol.*, 53(4), 539–544, doi:10.1093/icb/ict086, 2013.

Tomas, C. R. (ed): *Identifying Marine Phytoplankton*, Academic Press: San Diego, 858 pp., 1997.

Tortell, P. D., DiTullio, G. R., Sigman, D. M., and Morel, F. M. M.: CO₂ effects on taxonomic composition and nutrient utilization in an Equatorial Pacific phytoplankton assemblage, *Mar. Ecol. Prog. Ser.*, 236, 37–43, doi:10.3354/meps236037, 2002.

Trimborn, S., Wolf-Gladrow, D., Richter, K. U., and Rost, B.: The effect of pCO₂ on carbon acquisition and intracellular assimilation in four marine diatoms, *J. Exp. Mar. Bio. Ecol.*, 376(1), 26–36, doi:10.1016/j.jembe.2009.05.017, 2009.

Wijffels, S., Roemmich, D., Monselesan, D., Church, J., and Gilson, J.: Ocean temperatures chronicle the ongoing warming of Earth, *Nat. Clim. Chang.*, 6(2), 116–118, doi:10.1038/nclimate2924, 2016.

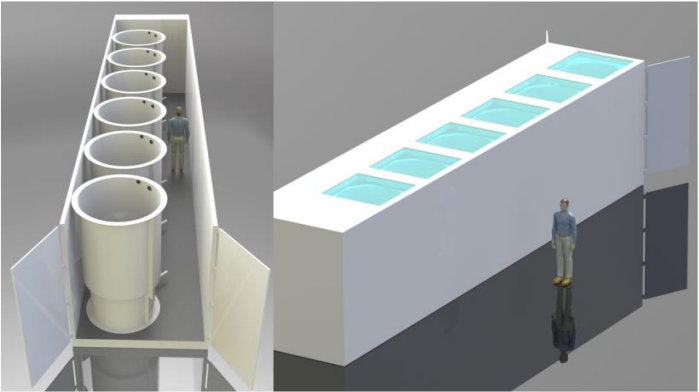
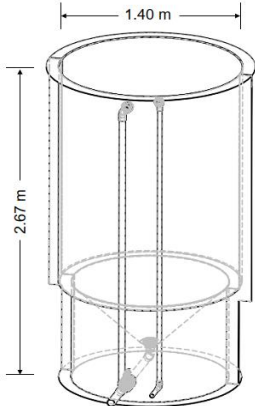
Wohlers, J., Engel, A., Zollner, E., Breithaupt, P., Jurgens, K., Hoppe, H.-G., Sommer, U. and Riebesell, U.: Changes in biogenic carbon flow in response to sea surface warming, *Proc. Natl. Acad. Sci.*, 106(17), 7067–7072, doi:10.1073/pnas.0812743106, 2009.

Wu, Y., Gao, K., and Riebesell, U.: CO₂-induced seawater acidification affects physiological performance of the marine diatom *Phaeodactylum tricornutum*, *Biogeosciences*, 7(9), 2915–2923, doi:10.5194/bg-7-2915-2010, 2010.

Yoshimura, T., Nishioka, J., Suzuki, K., Hattori, H., Kiyosawa, H., and Watanabe, Y. W.: Impacts of elevated CO₂ on organic carbon dynamics in nutrient depleted Okhotsk Sea surface waters, *J. Exp. Mar. Bio. Ecol.*, 395(1–2), 191–198, doi:10.1016/j.jembe.2010.09.001, 2010.

Yoshimura, T., Sugie, K., Endo, H., Suzuki, K., Nishioka, J., and Ono, T.: Organic matter production response to CO₂ increase in open subarctic plankton communities: Comparison of six microcosm experiments under iron-limited and -enriched bloom conditions, *Deep Res. Part I Oceanogr. Res. Pap.*, 94, 1–14, doi:10.1016/j.dsr.2014.08.004, 2014.

1166



1167

Field Code Changed

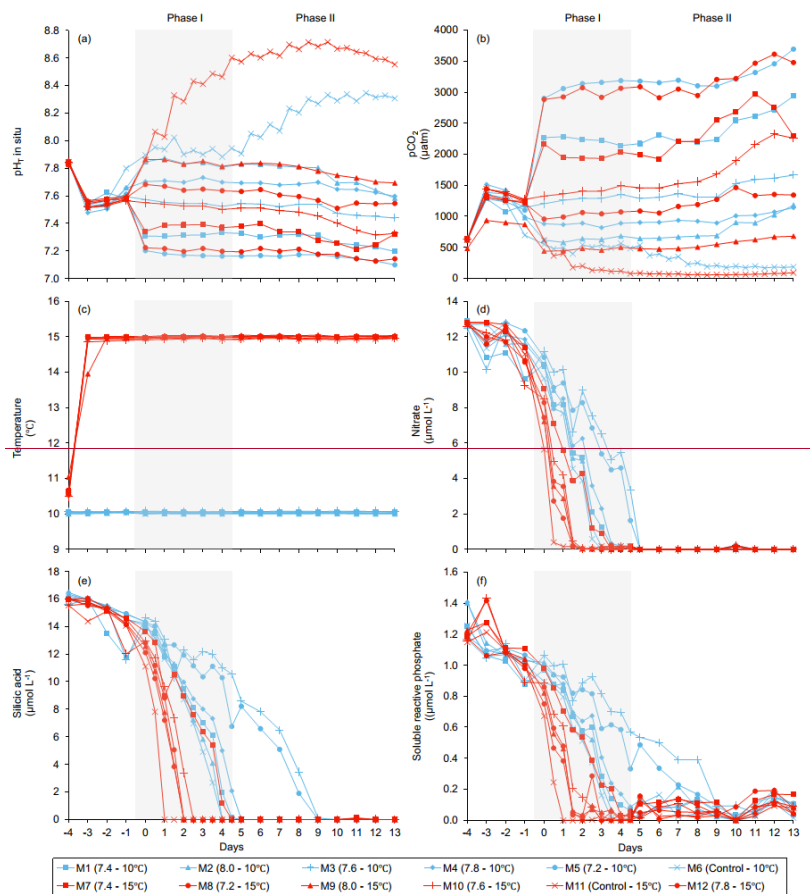
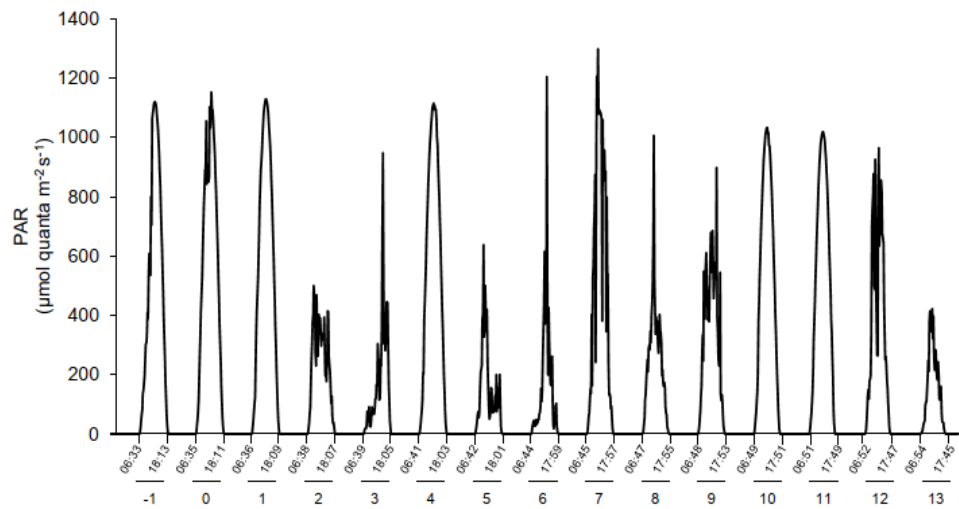


Figure 1. Schematic drawing including mesocosm dimensions and placement within the containers (Aquabiotech Inc, Québec, Canada). The whole setup includes a second container holding 6 more mesocosms not depicted here.

1172



Formatted: Normal

Field Code Changed

1173

1174

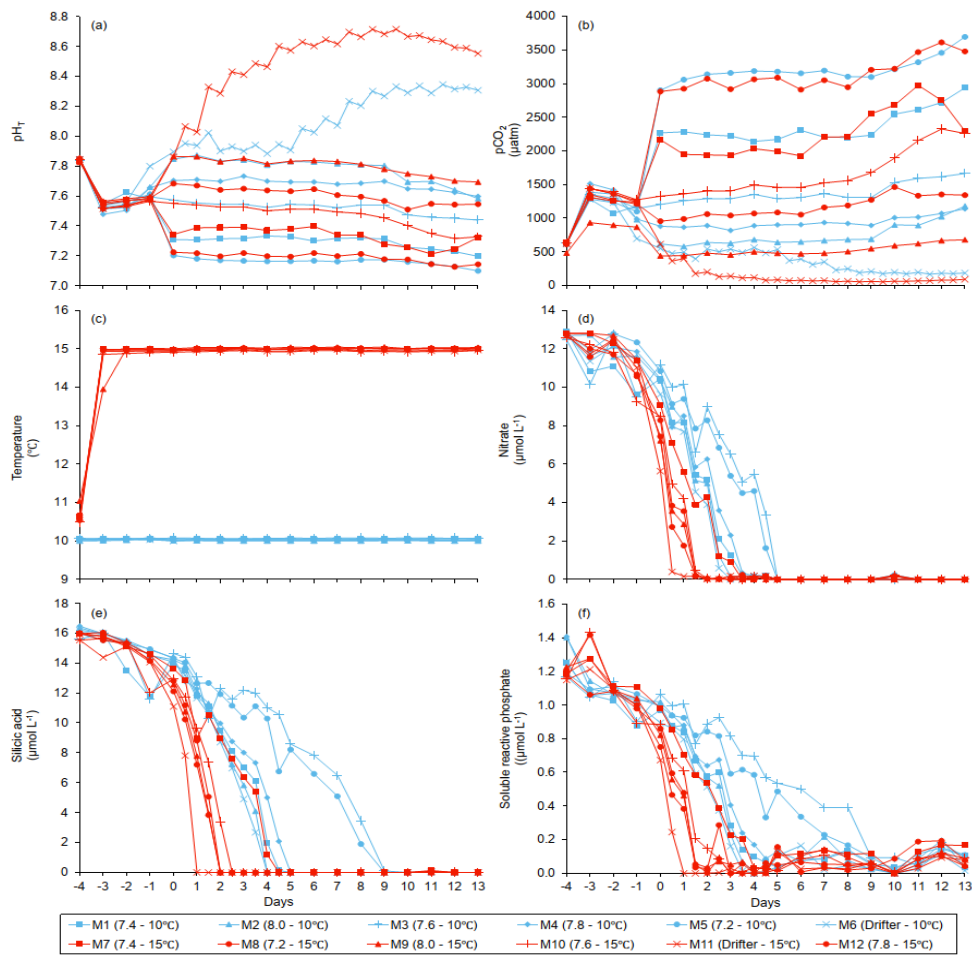
1175

1176

1177

Figure 2. Changes in incident photosynthetic active radiation (PAR) at the top of the mesocosms level during the experiment as measurement by a Satlantic HyperOCR hyperspectral radiometer and integrated in the 400-700 nm range. Local sunrise and sunset times (EDT) are indicated with the corresponding days of the experiment.

1178



1179

1180

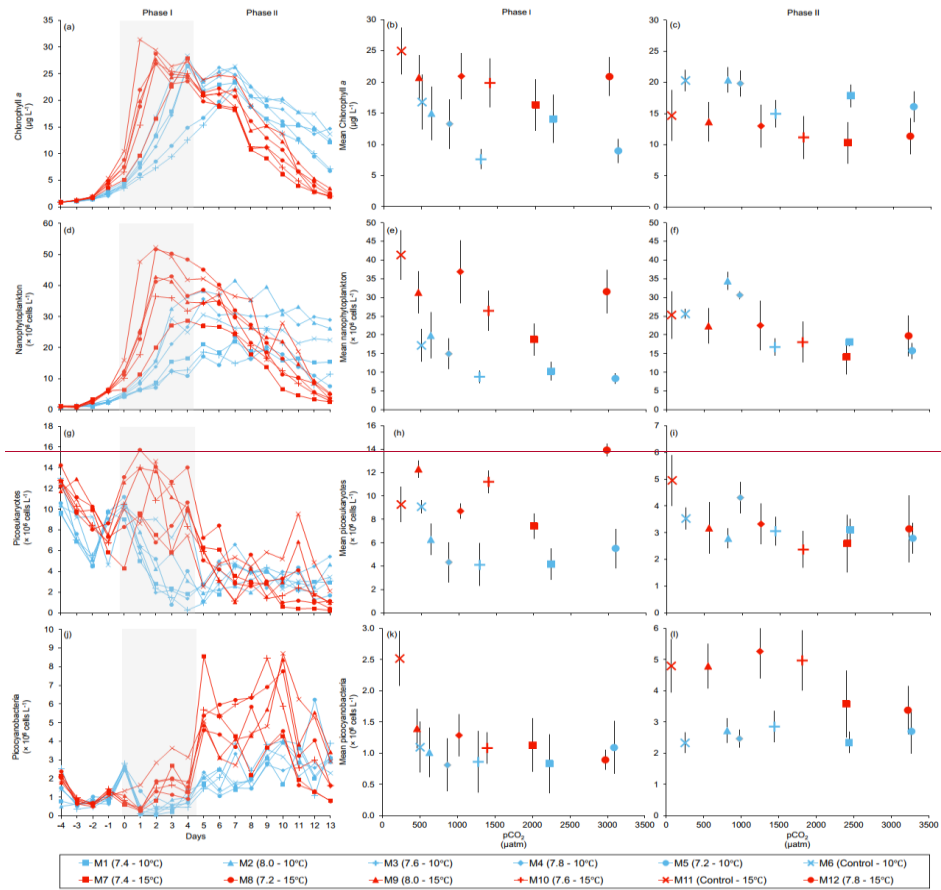
1181

1182

Figure 34. Temporal variations over the course of the experiment for: (a) pH_T, (b) pCO₂, (c) temperature, (d) nitrate, (e) silicic acid, (f) soluble reactive phosphate. For symbol attribution to treatments, see legend.

Formatted: Normal

Field Code Changed



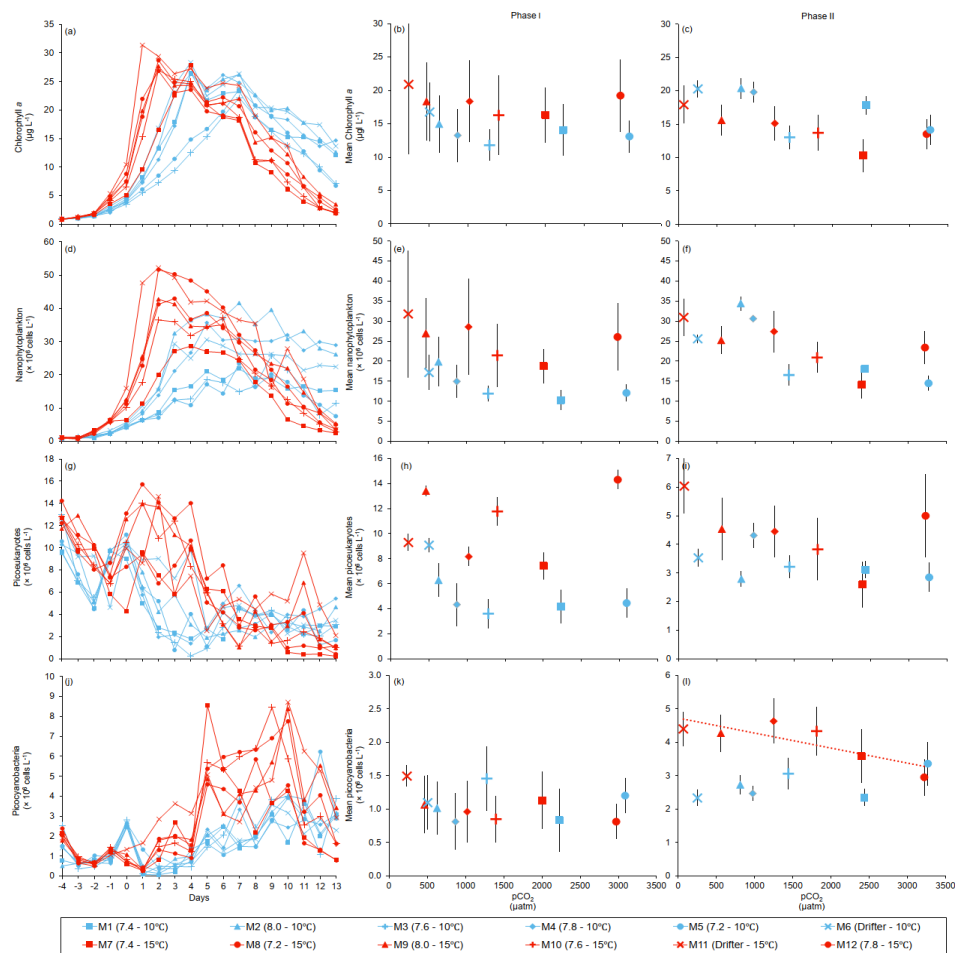
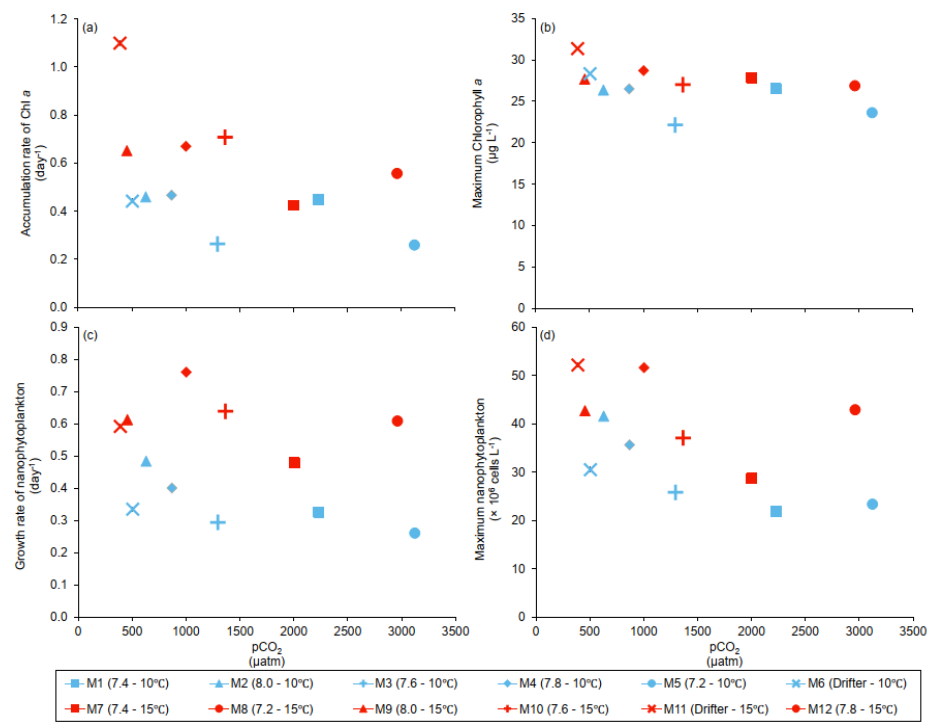


Figure 24. Temporal variations, and averages \pm SE during Phase I (day 0 to day of maximum Chl *a* concentration -4) and Phase II (day after maximum Chl *a* concentration -5 to day 13) for: (a-c) chlorophyll *a*, (d-f) nanophytoplankton, (g-i) picoeukaryotes, (j-l) picocyanobacteria. For symbol attribution to treatments, see legend.



Field Code Changed

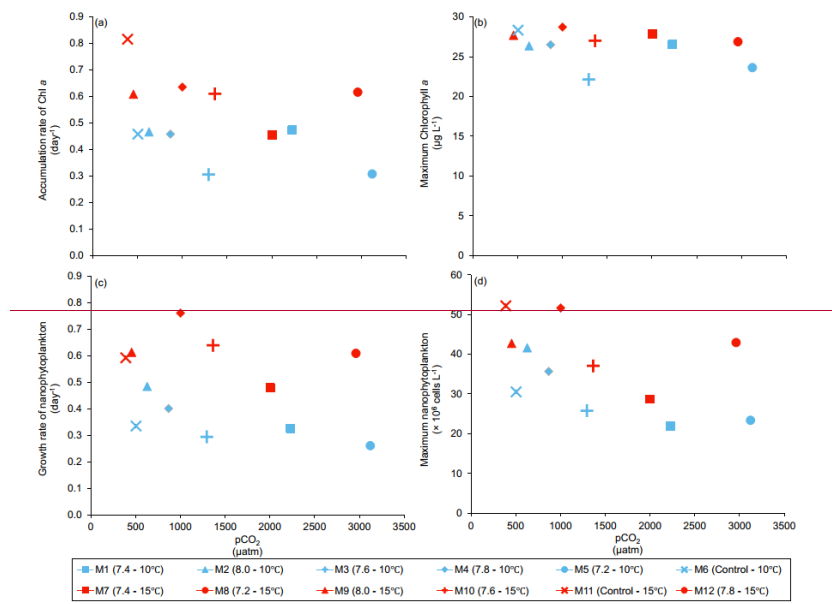
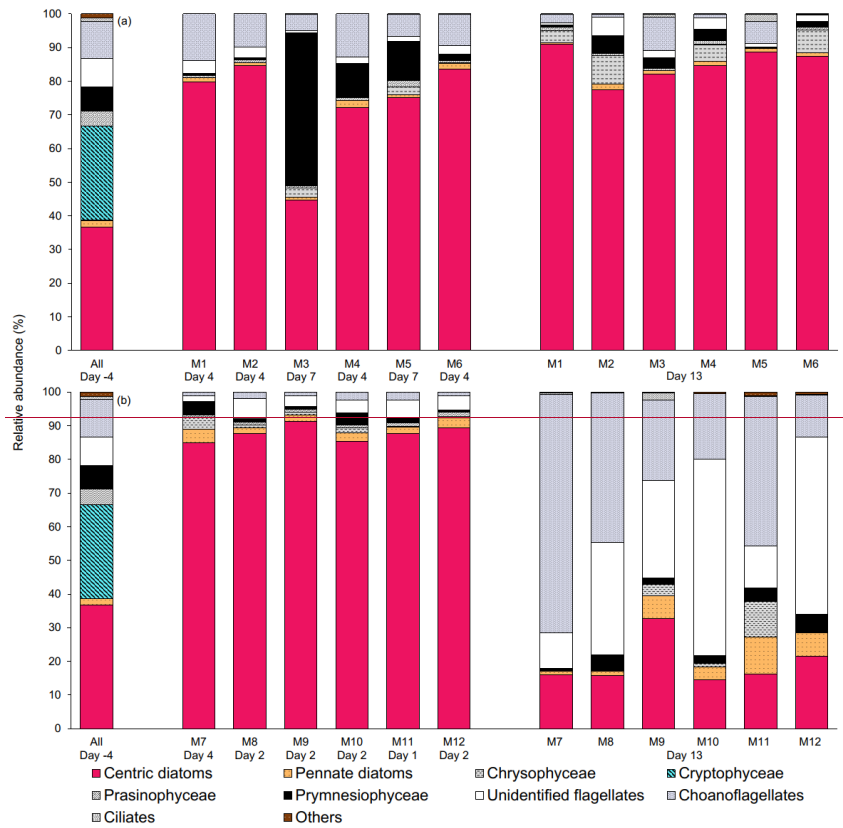


Figure 53. (a) Accumulation rate of Chl *a* (day 0 to maximum Chl *a* concentration), (b) maximum Chl *a* concentrations, (c) growth rate of nanophytoplankton (day 0 to maximum nanophytoplankton abundance), and (d) maximum nanophytoplankton abundance during the experiment. For symbol attribution to treatments, see legends.



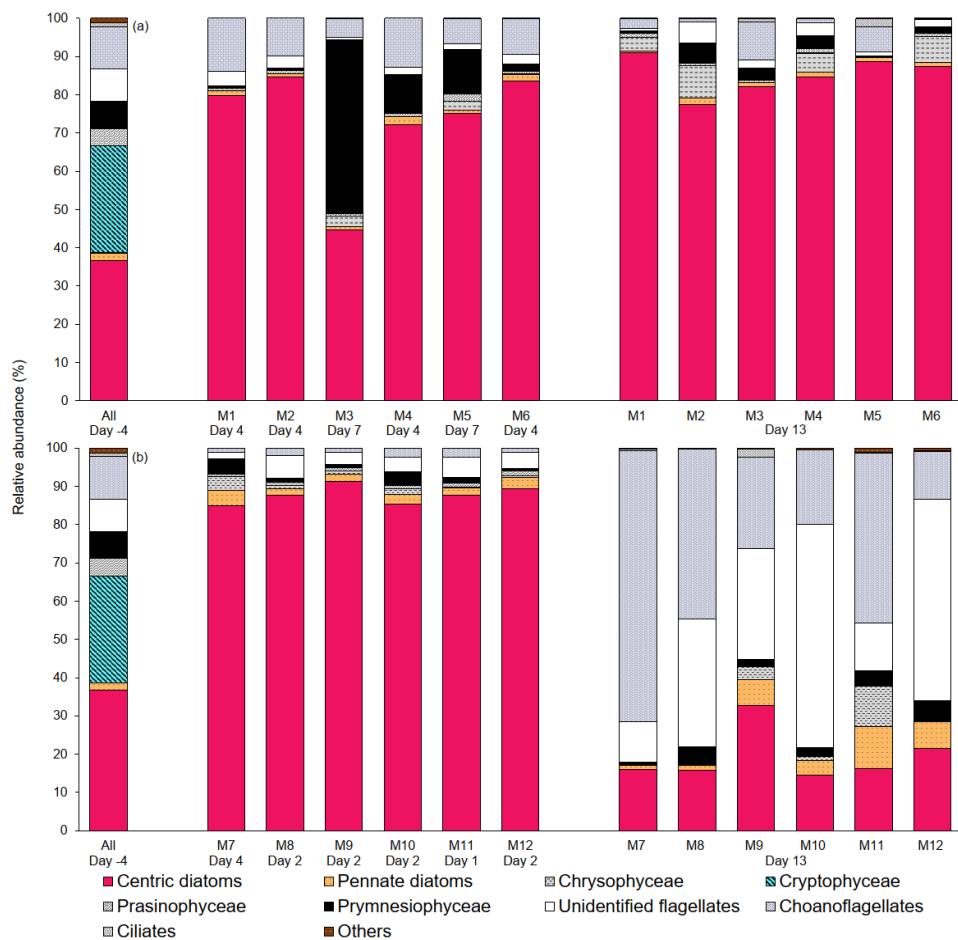
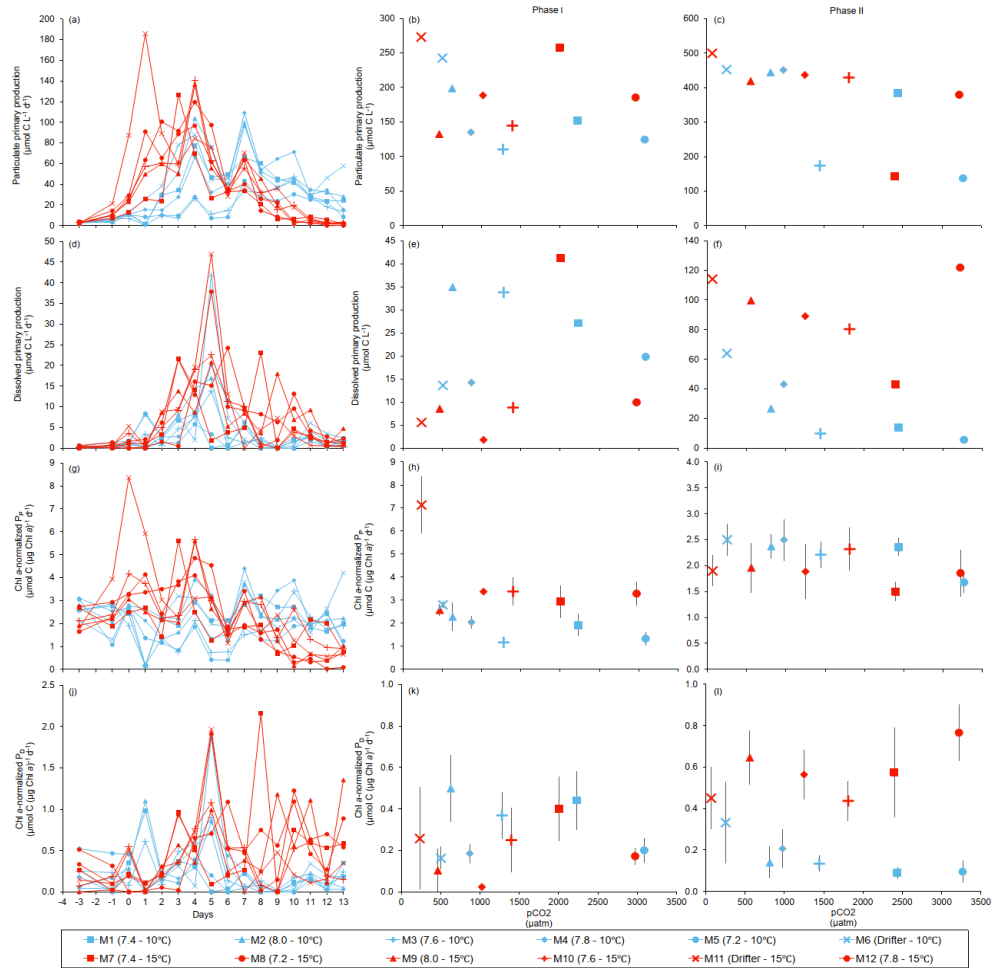


Figure 64. Relative abundance of 10 groups of protists at the beginning of the experiment (day -4), on the day of maximum Chl *a* concentrations in each mesocosm, and at the end of the experiment (day 13) for (a) 10 °C and (b) 15 °C mesocosms. The group « others » include dinoflagellates, Chlorophyceae, Dictyochophyceae, Euglenophyceae, heterotrophic groups, and unidentified cells. Each bar plot represents a mesocosm at a given time. The bar plot on day -4 represents the initial community assemblage before temperature manipulation and acidification, and is therefore the same for each temperature treatment. For symbol attribution to treatments, see legend.

Field Code Changed



Field Code Changed

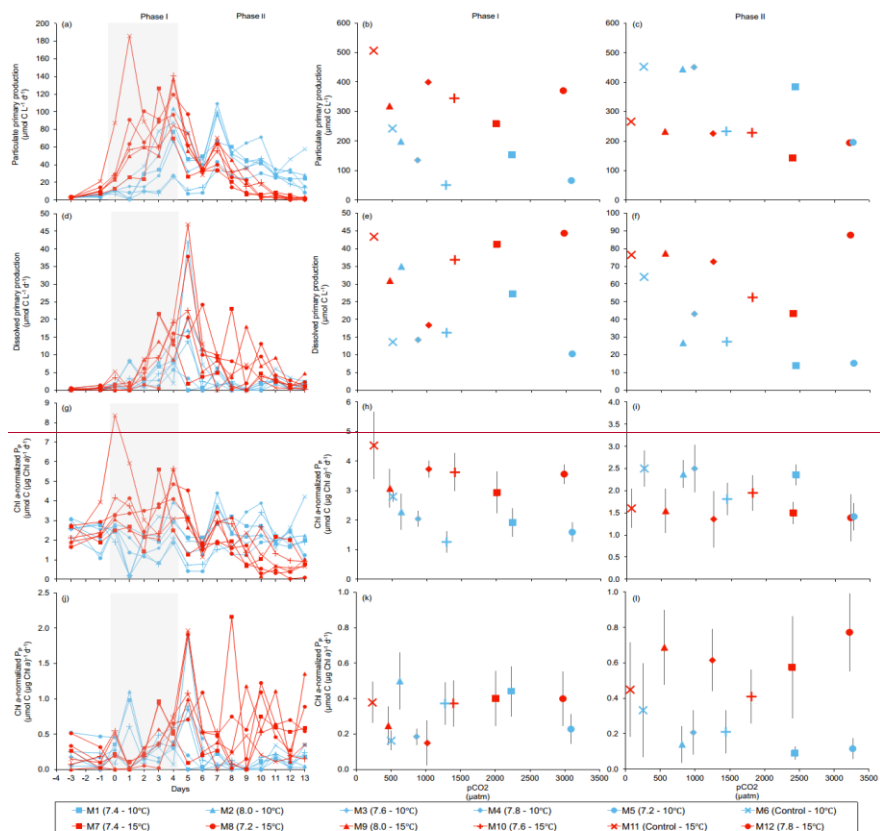
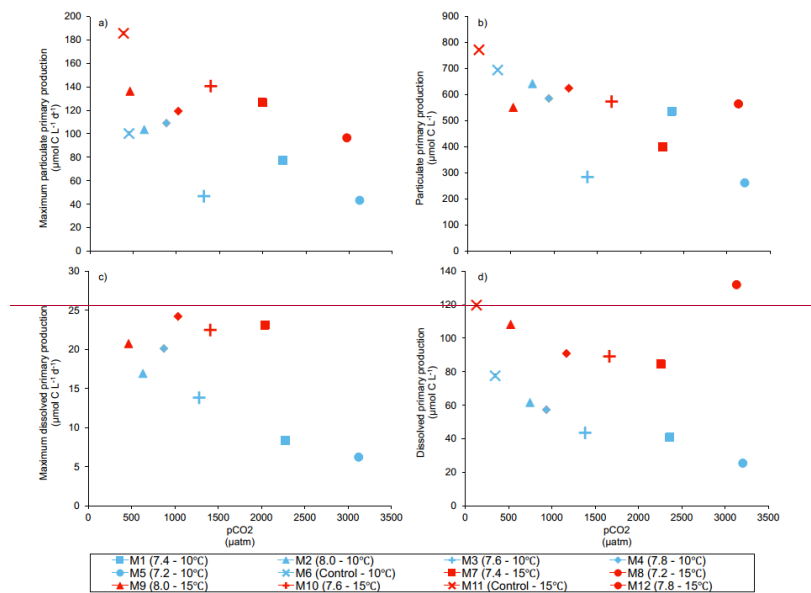


Figure 75. Temporal variations, time-integrated or averaged \pm SE during Phase I (day 0 to day of maximum Chl *a* concentration) and Phase II (day after maximum Chl *a* concentration to day 13) (day 0 to day 4) and Phase II (day 5 to day 13) for: (a-c) particulate primary production, (d-f) dissolved primary production, (g-i) Chl *a*-normalized particulate primary production, (j-l) Chl *a*-normalized dissolved primary production. For symbol attribution to treatments, see legend.



Field Code Changed

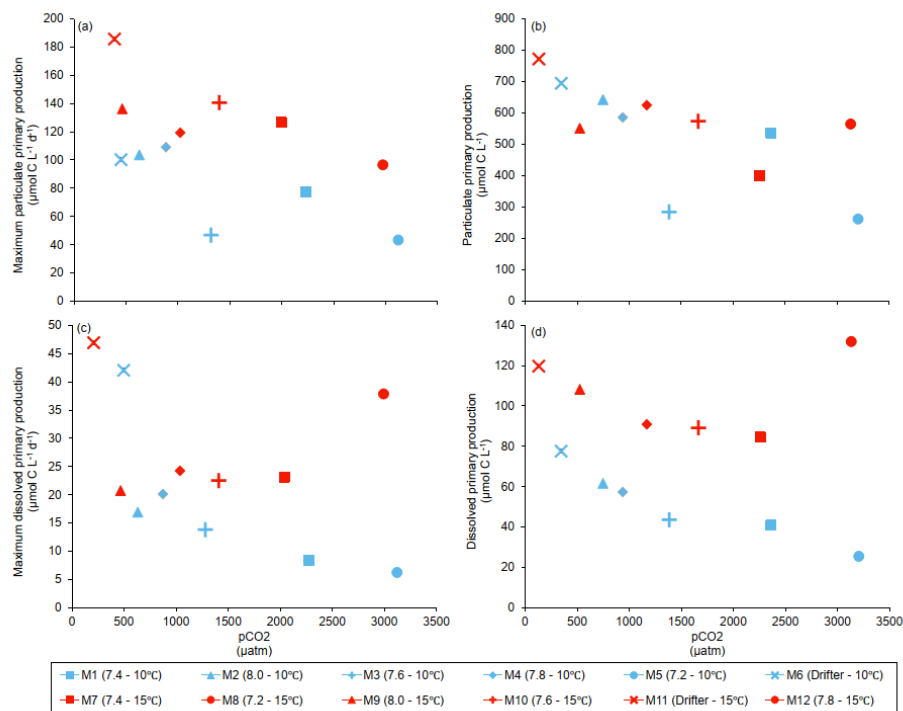


Figure 86. (a) Maximum particulate primary production, (b) time-integrated particulate primary production (c) maximum dissolved primary production, and (d) time-integrated dissolved primary production over the full course of the experiment (day 0 to day 13). For symbol attribution to treatments, see legend.

1221
1222
1223
1224

Table 1. Day of maximum Chl *a* concentration, the associated average pH_T (total hydrogen ion scale), and average pCO₂ over each individually defined phase. Phase I is defined from day 0 until day of maximum Chl *a* for each mesocosm, while Phase II is defined from the day after maximum Chl *a* until day 13. Average temperature over day 0 to day 13 is also presented for each mesocosm. Average values are presented with ± standard errors.

Mesocosm	Phase I		Phase II		Day 0–13	
	Day of max Chl <i>a</i>	pH _T	pCO ₂ (µatm)	pH _T	pCO ₂ (µatm)	Temperature (°C)
M1 (7.4 – 10 °C)	4	7.32 ± 0.01	2231 ± 25	7.28 ± 0.02	2437 ± 92	10.06 ± 0.01
M2 (8.0 – 10 °C)	4	7.84 ± 0.01	628 ± 16	7.74 ± 0.03	814 ± 65	10.00 ± 0.01
M3 (7.6 – 10 °C)	7	7.54 ± 0.01	1294 ± 18	7.48 ± 0.02	1503 ± 64	10.07 ± 0.01
M4 (7.8 – 10 °C)	4	7.71 ± 0.01	868 ± 13	7.66 ± 0.01	976 ± 29	10.04 ± 0.01
M5 (7.2 – 10 °C)	7	7.17 ± 0.01	3122 ± 35	7.15 ± 0.01	3315 ± 94	10.03 ± 0.01
M6 (Drifter – 10 °C)	4	7.93 ± 0.01	503 ± 15	8.22 ± 0.03	251 ± 25	10.02 ± 0.01
M7 (7.4 – 15 °C)	4	7.38 ± 0.01	2004 ± 44	7.31 ± 0.02	2399 ± 120	15.00 ± 0.01
M8 (7.2 – 15 °C)	2	7.21 ± 0.01	2961 ± 58	7.18 ± 0.01	3179 ± 74	15.01 ± 0.01
M9 (8.0 – 15 °C)	2	7.85 ± 0.01	454 ± 13	7.79 ± 0.02	545 ± 25	15.03 ± 0.01
M10 (7.6 – 15 °C)	2	7.54 ± 0.01	1364 ± 22	7.44 ± 0.02	1746 ± 106	14.94 ± 0.01
M11 (Drifter – 15 °C)	1	8.07 ± 0.01	388 ± 90	8.59 ± 0.02	84 ± 7	14.96 ± 0.02
M12 (7.8 – 15 °C)	2	7.67 ± 0.01	1001 ± 31	7.59 ± 0.01	1215.44 ±	14.98 ± 0.02

1225

1226
1227
1228
1229
1230
1231

Table 12. Results of the generalized least squares models (gls) tests for the effects of temperature, pCO₂, and their interaction during Phase I (day 0 to day of maximum Chl *a* concentration day 4). Separate analysis with pCO₂ as a continuous factor were performed when temperature had a significant effect. Chl *a* concentration, nanophytoplankton abundance, picoeukaryote abundance, picocyanobacteria abundance, particulate and dissolved primary production, and Chl *a*-normalized particulate and dissolved primary production. Significant results are in bold. *p < 0.05.

Response Variable	Factor	df	t-value	p-value
Mean Chl <i>a</i> concentration (µg L ⁻¹)	<u>Temperature</u>	<u>88</u>	<u>2.0042.3</u>	<u>0.0800.0</u>
	ure		07	50*
	<u>pCO₂</u>	<u>84</u>	<u>-0.464-</u>	<u>0.6550.2</u>
	pCO ₂ (10 °C)		1.362	45
	<u>pCO₂ ×</u>		<u>0.244-</u>	<u>0.8130.2</u>
Mean nanophytoplankton abundance (× 10 ⁶ cells L ⁻¹)	<u>Temperature</u>	<u>84</u>	<u>1.263</u>	<u>75</u>
	pCO ₂ (15 °C)			
	<u>Temperature</u>	<u>88</u>	<u>2.7252.9</u>	<u>0.026*0.</u>
	ure		80	018*
	<u>pCO₂ (10 °C)</u>	<u>44</u>	<u>-2.285-</u>	<u>0.0840.0</u>
Mean picoeukaryote abundance (× 10 ⁶ cells L ⁻¹)	pCO ₂ (10 °C)		2.729	53
	<u>pCO₂ (15 °C)</u>	<u>44</u>	<u>-1.191-</u>	<u>0.2990.2</u>
	pCO ₂ (15 °C)		1.231	86
	<u>Temperature</u>	<u>88</u>	<u>1.0561.1</u>	<u>0.3220.2</u>
	ure		57	81
Mean picocyanobacteria abundance (× 10 ⁶ cells L ⁻¹)	<u>pCO₂</u>	<u>88</u>	<u>-1.159-</u>	<u>0.2800.3</u>
	pCO ₂		1.070	16
	<u>pCO₂ ×</u>		<u>1.1251.0</u>	<u>0.2930.3</u>
	<u>Temperature</u>	<u>88</u>	<u>1.1251.0</u>	<u>0.2930.3</u>
	Temperature ×		85	09
Mean picocyanobacteria abundance (× 10 ⁶ cells L ⁻¹)	<u>Temperature</u>	<u>88</u>	<u>0.8913.0</u>	<u>0.3990.0</u>
	ure		66	15*
	<u>pCO₂</u>	<u>84</u>	<u>0.9910.1</u>	<u>0.3510.9</u>
	pCO ₂ (10 °C)		25	07

Formatted Table

Particulate primary production ($\mu\text{mol C L}^{-1}$)	$\frac{\text{pCO}_2}{\text{Temperature}} \times$		
	$\frac{\text{pCO}_2}{\text{Temperature}} \times$	84	-1.166- 0.2770.0
	(15 °C)		2.268 86
	$\frac{\text{pCO}_2}{\text{Temperature}} \times$		-
	$\frac{\text{pCO}_2}{\text{Temperature}} \times$	88	0.1242.6 0.9050.0
	(10 °C)		28*
	$\frac{\text{pCO}_2}{\text{Temperature}} \times$	84	-1.011- 0.3420.1
	(15 °C)		1.617 81
	$\frac{\text{pCO}_2}{\text{Temperature}} \times$	84	0.867- 0.4110.3
	(15 °C)		0.992 78
	$\frac{\text{pCO}_2}{\text{Temperature}} \times$	88	-
	(10 °C)		1.4290.7 0.1910.4
Dissolved primary production ($\mu\text{mol C L}^{-1}$)	$\frac{\text{pCO}_2}{\text{Temperature}} \times$	88	-0.569- 0.5850.3
	(10 °C)		0.901 94
	$\frac{\text{pCO}_2}{\text{Temperature}} \times$	88	0.7230.9 0.4900.3
	(10 °C)		56 67
	$\frac{\text{pCO}_2}{\text{Temperature}} \times$	88	1.6892.5 0.1300.0
	(10 °C)		92 32*
	$\frac{\text{pCO}_2}{\text{Temperature}} \times$	84	0.107- 0.9180.2
	(10 °C)		1.467 16
	$\frac{\text{pCO}_2}{\text{Temperature}} \times$	84	-0.381- 0.7130.4
	(15 °C)		0.840 48
	$\frac{\text{pCO}_2}{\text{Temperature}} \times$	88	-1.046- 0.3260.7
	(10 °C)		0.350 35
Chl <i>a</i> -normalized particulate primary production ($\mu\text{mol C } (\mu\text{g Chl } a)^{-1} \text{ d}^{-1}$)	$\frac{\text{pCO}_2}{\text{Temperature}} \times$	88	-0.381- 0.7130.7
	(10 °C)		0.397 02
Chl <i>a</i> -normalized dissolved primary production ($\mu\text{mol C } (\mu\text{g Chl } a)^{-1} \text{ d}^{-1}$)	$\frac{\text{pCO}_2}{\text{Temperature}} \times$	88	-0.381- 0.7130.7
	(10 °C)		0.397 02

1232

ρ_{CO_2}	x		
Temperature	ρ_{CO_2}	88	0.4490-5 0.6650-6
Temperature		22	46

1233
1234
1235
1236

Table 32. Results of the generalized least squares models (gls) tests for the effects of temperature, pCO₂ and their interaction. Separate analysis with pCO₂ as a continuous factor were performed when temperature had a significant effect. Accumulation rate of Chl *a* (day 0 to maximum Chl *a* concentration), maximum Chl *a* concentration, growth rate of nanophytoplankton (day 0 to maximum nanophytoplankton abundance), and maximum nanophytoplankton abundance. Significant results are in bold. *p < 0.05.

Response Variable	Factor	df	t-value	p-value
Accumulation rate of Chl <i>a</i> (day ⁻¹)	Temperature	8	2.679	0.028*
	pCO ₂ (10 °C)	4	-1.476	0.214
	pCO ₂ (15 °C)	4	-1.759	0.154
	Temperature	8	1.305	0.228
Maximum Chl <i>a</i> concentration (µg L ⁻¹)	pCO ₂	8	-0.387	0.709
	pCO ₂ × Temperature	8	0.022	0.983
	Temperature	8	2.534	0.035*
Growth rate of nanophytoplankton (day ⁻¹)	pCO ₂ (10 °C)	4	-0.882	0.403
	pCO ₂ (15 °C)	4	0.601	0.564
	Temperature	8	1.380	0.205
Maximum nanophytoplankton abundance (× 10 ⁶ cells L ⁻¹)	pCO ₂	8	-0.735	0.484
	pCO ₂ × Temperature	8	0.302	0.770
	Temperature	8	1.380	0.205

1237

Formatted: Left

Formatted Table

Formatted: Left

Formatted: Left

Formatted: Left

Formatted: Left

Particulate primary production ($\mu\text{mol C L}^{-1}$)	Temperature Temperature	88	-0.015- 2.248	0.9880.012 *
	pCO₂ pCO ₂ (10 °C)	84	-0.940- 2.186	0.3750.094
	pCO₂ x			
	Temperature pCO ₂ (15 °C)	84	0.460- 2.390	0.6580.075
Dissolved primary production ($\mu\text{mol C L}^{-1}$)	Temperature Temperature	88	1.8941- 154	0.0950.282
	pCO₂ pCO ₂	88	-1.145- 1.701	0.2850.127
	pCO₂ x			
	Temperature pCO ₂ x Temperature	88	0.8471- 369	0.4220.208
(Log) Chl <i>a</i>-normalized, particulate primary production ($\mu\text{mol C (}\mu\text{g Chl } a)^{-1} \text{ d}^{-1}$)Chl <i>a</i>- normalized particulate primary production ($\mu\text{mol C (}\mu\text{g Chl } a)^{-1} \text{ d}^{-1}$)	Temperature Temperature	88	-2.288- 3.387	0.0520.010 **
	pCO₂ pCO ₂ (10 °C)	84	-1.491- 2.226	0.1740.090
	pCO₂ x			
	Temperature pCO ₂ (15 °C)	84	1.105- 0.366	0.3010.733
(Log) Chl <i>a</i>-normalized, dissolved primary production ($\mu\text{mol C (}\mu\text{g Chl } a)^{-1} \text{ d}^{-1}$)Chl <i>a</i>- normalized dissolved primary production ($\mu\text{mol C (}\mu\text{g Chl } a)^{-1} \text{ d}^{-1}$)	Temperature Temperature	88	2.3571- 973	0.046*0.07 3
	pCO₂ (10 °C) pCO ₂	48	-2.573- 1.838	0.0620.103
	pCO₂ (15 °C) pCO ₂ x Temperature	48	1.3451- 860	0.2500.100

Formatted: Left, Widow/Orphan control

Formatted: Left, Widow/Orphan control

Formatted: Left

Formatted: Left, Widow/Orphan control

Formatted: Left, Widow/Orphan control

Formatted: Left, Widow/Orphan control

Formatted: Left

Formatted: Left, Widow/Orphan control

Formatted: Font: Times New Roman, English (Canada)

Formatted: Left

Formatted: Font: Times New Roman, Font color: Auto, English (Canada)

Formatted: Left, Widow/Orphan control

Formatted: Font: Times New Roman, English (Canada)

Formatted: Left

Formatted: Font: Times New Roman, Font color: Auto, English (Canada)

Formatted: Left, Widow/Orphan control

Formatted: Left, Widow/Orphan control

Formatted: Left, Widow/Orphan control

1244
1245
1246
1247

Table 54. Results of the generalized least squares models (gls) tests for the effects of temperature, pCO₂ and their interaction. Separate analysis with pCO₂ as a continuous factor were performed when temperature had a significant effect. Maximum particulate and dissolved primary production, and time-integration over the full duration of the experiment (day 0 to day 13). Natural logarithm transformation is indicated in parentheses when necessary, significant results are in bold. *p < 0.05, **p < 0.01.

Response Variable	Factor	df	t-value	p-value
Maximum particulate primary production (μmol C L ⁻¹ d ⁻¹)	Temperature	8	2.466	0.039*
	pCO ₂ (10 °C)	4	-2.328	0.080
	pCO ₂ (15 °C)	4	-2.394	0.075
Time-integrated particulate primary production (μmol C L ⁻¹ d ⁻¹)	Temperature	8	-0.055	0.958
	pCO ₂ (10 °C)	4	-1.300	0.230
	pCO ₂ (15 °C)	4	0.801	0.446
(Log) Maximum dissolved primary production (μmol C L ⁻¹)	Temperature	8	-0.659	0.528
	pCO ₂	8	-3.342	0.010**
	pCO ₂ × Temperature	8	2.858	0.021*
Time-integrated dissolved primary production (μmol C L ⁻¹)	Temperature	8	1.687	0.130
	pCO ₂	8	-2.153	0.063
	pCO ₂ × Temperature	8	1.880	0.097

1248

Formatted: Widow/Orphan control

Formatted Table

Formatted: Widow/Orphan control

Formatted: Widow/Orphan control

Formatted: Widow/Orphan control

Formatted: Widow/Orphan control